

Model Based Evaluation of UEGO Performance and Sensitivity

Master's thesis
performed in **Vehicular Systems**

by
Tommy Jakobsson

Reg nr: LiTH-ISY-EX -- 06/3963 -- SE

January 4, 2007

Model Based Evaluation of UEGO Performance and Sensitivity

Master's thesis

performed in **Vehicular Systems,**
Dept. of Electrical Engineering
at **Linköpings universitet**

by **Tommy Jakobsson**

Reg nr: LiTH-ISY-EX -- 06/3963 -- SE

Supervisor: **Per Öberg**

Examiner: **Associate Professor Lars Eriksson**

Linköping, January 4, 2007

Presentationsdatum 06-12-21 Publiceringsdatum 06-12-28	Institution Division of Vehicular System Department of Electrical Engineering Linköpings Universitet SE-581 83 Linköping	 Linköpings universitet
Språk ____ Svenska <input checked="" type="checkbox"/> English Antal sidor 81	Typ av publikation ____ Licentiatavhandling ____ Rapport <input checked="" type="checkbox"/> Examensarbete ____ C-uppsats ____ D-uppsats	ISBN - ISRN LiTH-ISY-EX--06/3963 Serietitel (Licentiatavhandling) - Serienr/ISSN(Licentiatavhandling) -
URL http://www.ep.liu.se http://www.vehicular.isy.liu.se		
Publikationens titel Model Based Evaluation of UEGO Performance and Sensitivity Modellbaserad utvärdering utav prestanda och känslighet hos en UEGO Författare: Thommy Jakobsson		
Abstract Closed loop fuel injection has been in use for two decades but it's not until the recent five years that the wide band lambda sensor have been utilized. The goal is to explain wide band and discrete lambda sensors in a simple but powerful way. Both sensors are modeled by simple mathematics and accounts for Oxygen, Hydrogen and Carbon monoxide influences. The focus is not just on the output from the sensors, but also on the underlying function. This means that all explanations are thorough and methodical. The function of a wide band lambda sensor is more complicated than a discrete type lambda sensor, therefore it's harder to get correct readings. The model of the wide band lambda sensor is used to evaluate different problems in preparation for the development of an observer. Several potential problem sources are tested and investigated; these include calibration error, pressure error, air leak error, gas sensitivity and fuel errors. To evaluate the potential problems and their ability to explain differences between actual lambda and sensor output, two sensors with differing outputs have been used. The final result is implemented in an ECU. The models indicate that the difference between the two sensors is most likely explained by different sensitivity for CO, O2 and H2. This can in turn have one or several explanations. It is suggested that different ability to pump oxygen, different nernst cells or even different controllers can cause this. The reason is not investigated further as this would require a very deep research on the two sensors. Because no usable explanation is found an observer that estimates the offset at stoichiometric conditions, where lambda equals one, is constructed. The observer uses the fact that the switch point of a discrete lambda sensor is insensitive to disturbances. The offset calculation is performed in real time on an ECU. Tools for calibration of the observer are also developed. With the observer the error for the two sensors is roughly halved over the whole spectrum and at stoichiometric conditions, which is the normal operation for an engine, the error was too small to measure. Although the wide band lambda sensor is a very complex sensor it is shown that it can be understood with simple mathematics and basic knowledge in chemistry. The developed model agrees well with the real sensor for steady state conditions. For transient conditions, however, the model needs to be refined further. The question why the two sensors differ is discussed but the true origin of the cause remains unsolved. The conclusion is that the error can be drastically reduced with just an offset. It is also shown that when building a lambda sensing device the controller is of equal importance as the sensor element itself. This is due to the sensitivity of surrounding factors that the controller must be able to handle. These effects are specially important for engines running at lambda not equal to 1, for example diesel engines.		
Keywords: wide band, uego, ego, o2 sensor, oxygen sensor, lambda		

Abstract

Closed loop fuel injection has been in use for two decades but it's not until the recent five years that the wide band lambda sensor have been utilized. The goal is to explain wide band and discrete lambda sensors in a simple but powerful way. Both sensors are modeled by simple mathematics and accounts for Oxygen, Hydrogen and Carbon monoxide influences. The focus is not just on the output from the sensors, but also on the underlying function. This means that all explanations are thorough and methodical. The function of a wide band lambda sensor is more complicated than a discrete type lambda sensor, therefore it's harder to get correct readings. The model of the wide band lambda sensor is used to evaluate different problems in preparation for the development of an observer. Several potential problem sources are tested and investigated; these include calibration error, pressure error, air leak error, gas sensitivity and fuel errors. To evaluate the potential problems and their ability to explain differences between actual lambda and sensor output, two sensors with differing outputs have been used. The final result is implemented in an ECU.

The models indicate that the difference between the two sensors is most likely explained by different sensitivity for CO, O₂ and H₂. This can in turn have one or several explanations. It is suggested that different ability to pump oxygen, different nernst cells or even different controllers can cause this. The reason is not investigated further as this would require a very deep research on the two sensors. Because no usable explanation is found an observer that estimates the offset at stoichiometric conditions, where lambda equals one, is constructed. The observer uses the fact that the switch point of a discrete lambda sensor is insensitive to disturbances. The offset calculation is performed in real time on an ECU. Tools for calibration of the observer are also developed. With the observer the error for the two sensors is roughly halved over the whole spectrum and at stoichiometric conditions, which is the normal operation for an engine, the error was too small to measure.

Although the wide band lambda sensor is a very complex sensor it is shown that it can be understood with simple mathematics and basic knowledge in chemistry. The developed model agrees well with the real sensor for steady state conditions. For transient conditions, however, the model needs to be refined further. The question why the two sensors differ is discussed but the true origin of the cause remains unsolved. The conclusion is that the error can be drastically reduced with just an offset. It is also shown that when building a lambda sensing device the controller is of equal importance as the sensor element itself. This is due to the sensitivity of surrounding factors that the controller must be able to handle. These effects are specially important for engines running at lambda not equal to 1, for example diesel engines.

Keywords: wide band, narrow band, switch type, uego, ego, o₂ sensor, oxygen sensor, lambda, zirconia

Preface

This master's thesis has been performed at Vehicular Systems at Linköpings Universitet, Sweden, during the period from January to October 2006.

Acknowledgment

First of all I would like to thank my supervisor Per Öberg Ph.D. student for his generously spent hours to help. Also I would like to thank my examiner Associate Prof. Lars Eriksson. Special thanks to the Research engineer Martin Gunnarsson for his technical help in the laboratory. Last but not least I would like to thank my beloved Camilla for all her love, care and support.

Notation

Symbols and acronyms used in the report.

Variables and parameters

$[XX]$	Concentration of XX
$\alpha, \beta, \gamma, \delta, \epsilon$	Constants
A	Area
c	concentration fraction, Taylor coefficients
e	electron charge
E	Potential, Energy
F	Faradays constant
I, i	Current
θ	Occupancies
ϑ	fraction
k	Constant
K	Equilibrium constant
λ	lambda value, mixture strength
L	Adsorption capacity
μ	Potential
m	Mass, Mass transfer
M	Mole mass
N, n	Number of
ξ	Progress, Parameterization
R	Resistance, Gas constant
r	rate
T	Temperature
t	Time in seconds
U	Output
V	Voltage
v	Stoichiometric constant, Vacancies
y	Constant

Modifiers

0	Standard conditions
$'$	Modified
x	of x
\cdot	rate of

Acronyms

A/F	Air to Fuel
AC	Alternating Current
CNG	Compressed Natural Gas
ECU	Engine Control Unit
EGO	Exhaust Gas Oxygen
RPM	Revolutions Per Minute
UEGO	Universal Exhaust Gas Oxygen

Contents

Abstract	III
Preface and Acknowledgment	V
Notation	VII
Contents	IX
1 Introduction	1
1.1 Purpose	1
1.2 Method and Outline	1
1.3 Emissions from a Gasoline engine	1
1.3.1 Lambda (λ)	2
1.3.2 Pollutants	2
1.4 Environmental Legislation	3
1.5 Progress	4
1.5.1 Fuel Injection	5
1.5.2 Catalytic Converters	5
1.5.3 Lambda sensor	5
1.6 Engine setup	6
1.7 Reading Instructions	6
2 Prerequisites	7
2.1 Engine	7
2.1.1 Physical	7
2.1.2 Operation	7
2.1.3 Intake	8
2.1.4 Turbo	8
2.2 Chemistry	9
2.2.1 Chemical equilibrium	9
2.3 Thermodynamics	9
2.4 Electro chemistry	10
3 Lambda sensors	11
3.1 Switch type	11
3.1.1 Physical structure	11
3.1.2 Zirconia sensor	12
3.1.3 Titania sensor	13
3.1.4 Evaluation of sensor	13
3.2 Wide band	14
3.2.1 Physical structure	14
3.2.2 Function	14
3.2.3 Evaluation of sensor	15

4	UEGO Model	18
4.1	Data	18
4.1.1	Exhaust model	18
4.2	Switch type model	20
4.2.1	Nernst equation	21
4.2.2	Linear Regression models	21
4.2.3	Full Auckenthaler	23
4.2.4	Simplified Auckenthaler	26
4.2.5	Simplified Auckenthaler with diffusion	26
4.3	Diffusion	28
4.3.1	Results	28
4.4	Oxygen Pump	28
4.4.1	Results	29
4.5	Regulator	29
4.5.1	Results	29
4.6	Lambda generation	29
4.6.1	Brettschneider	30
4.6.2	Lookup table	30
4.6.3	Conclusion	31
5	Validation of wide band model	34
5.1	Test setup	34
5.2	Testing of the model	34
5.2.1	Calibration	34
5.2.2	Exhaust gas Model	34
5.2.3	Real Test Data	34
5.2.4	Results	35
5.3	Pressure	35
5.3.1	Results	35
5.4	Temperature	36
5.5	Improvement of UEGO model	36
5.5.1	Diffusion	36
5.5.2	More data	36
5.5.3	More gases	36
5.5.4	Better pressure tests	36
6	Observer	39
6.1	Problem	39
6.1.1	Exhaust gas model tests	39
6.1.2	R_{cat} error	39
6.1.3	Pressure error	40
6.1.4	Temperature error	41
6.1.5	Air leaks error	41
6.1.6	Different gas sensitivity error	41
6.1.7	Fuel difference error	42
6.1.8	Conclusion	42
6.2	Solution	43
6.3	Matlab/Simulink Model	43
6.3.1	Observer Model	43
6.3.2	Running Average Model	43
6.3.3	Results	44
6.4	Implemented model	44
7	Validation of UEGO observer	49
7.1	Adaption	49
7.2	Force lambda swing	49
7.3	Conclusions	50

8	Final thoughts and Conclusions	52
8.1	Correctness of UEGO model	52
8.2	Guidelines for a optimal UEGO	52
8.3	Guidelines for an optimal use	52
8.4	Differing lambda	52
8.5	Observer	53
References		54
A	Data	58
A.1	Problems with test data	58
A.2	Structure and data	58
B	Calculated values	62

Chapter 1

Introduction

Already in 1306 King Edward I banned coal fires in London, the reason were complains from the upper-class about smog. The law did never get any real impact and was soon removed[7] but today smog is once again a big problem. Although nowadays it's hardly coal fires that causes smog in London, the car is. When the first petrol driven automobile was introduced in USA in the late 1880s there where already much talk about the environmental influence. Ironically, considering the knowledge of today, the introduction of the automobile was seen upon as a environmental improvement over horses. The reason was horse manure, in New York City alone over 10,000 tons of manure had to be removed from the streets daily [17]. At that time no one could hardly have predicted the automobile's future, it's success and the environmental disaster that was soon to follow. Only in 2005 63 million cars and light trucks were delivered around the world and the dramatic increase is expected to continue for at least the next three decades. Nature is already suffering tremendously and in the end, as always, human health will suffer. Not only is the car today recognized as the main source for pollution but also for noise and high cost with todays constantly increasing gasoline prices. Since the 70s, legislation have demanded harder and harder restrictions for pollutants produced by a car and also noise and recycling of the car itself. This chapter will give a short introduction to the work.

1.1 Purpose

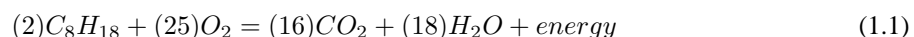
The purpose of this thesis is to investigate and explore lambda sensors and find reasons why seemingly correct sensors can have differing outputs. If an explanation is found, or an equally good idea to improve sensor readings, an observer for lambda will be constructed.

1.2 Method and Outline

Several models are described and tested against a real sensor output. The result is evaluated to find a suitable model, this can be found in chapter 4. These models are used to evaluate six kinds of errors in chapter 6. The knowledge gained is used to construct an observer.

1.3 Emissions from a Gasoline engine

When burning hydrocarbons ideally you get water (H_2O) and carbon-dioxide(CO_2). For example gasoline, which often is simplified to be octane (C_8H_{18}), has the following ideal chemical reaction when burned:



In reality this equation is never satisfied and an *incomplete reaction* will occur. This is mainly due to two reasons:

- First of all the fuel is never entirely pure causing an imperfect combustion.
- Secondly, the combustion has a limited set of time in the combustion chamber (i.e cylinder) resulting in a non-homogeneous mixture. This in turn results in some hydrocarbons never get in contact with air or get enough heat to participate.

The results from the incomplete reaction is carbon-oxide(CO), hydrogen(H_2) and hydrocarbons (C_xH_y) commonly known as HC . When burning hydrocarbons in an engine air is used instead of pure oxygen, i.e. large amount of nitrogen is present. Although we never see that nitrogen oxidize in nature there is an equilibrium involving oxygen, nitrogen and it's oxides. In normal air-temperature the equilibrium is so far shifted towards pure oxygen and nitrogen so we never observe any nitrogen-oxide. In an engine on the other hand the temperature is far higher and various types of nitrogen-oxides is created. These gases is never allowed to reach complete chemical equilibrium again resulting in emissions collected under the name NO_x . Actually the name is a bit misleading because N_xO is also included. These gases are however created in extremely low concentrations suggestion the merge.

1.3.1 Lambda (λ)

To be able to freely discuss emissions lambda must first be defined. Without going into details a gasoline engine needs air and it needs fuel to run. If *air-to-fuel ratio*(A/F) is defined as:

$$(A/F) = \frac{m_a}{m_f} \quad (1.2)$$

Where m_a and m_f is the mass of air respective the fuel entering the engine. Lambda is then defined as:

$$\lambda = \frac{(A/F)}{(A/F)_s} \quad (1.3)$$

Where $(A/F)_s$ is the so called *stoichiometric air-to-fuel ratio* and is the air-to-fuel ratio when a complete reaction (theoretically) occurs. When $\lambda > 1$ the mixture is called lean and likewise when $\lambda < 1$ the mixture is called rich. Traditionally ϕ has been used by some engineers, where $\phi = \frac{1}{\lambda}$.

1.3.2 Pollutants

Several of the gases produced by an engine is poisonous for humans. Figure 1.1 shows the resulting concentration, under equilibrium, for different ϕ . The Figure shows the concentrations under three different temperatures, it's clear that lower temperature means higher variations of concentrations. Observe that the fraction NO_x increases rapidly with higher temperature.

Carbon monoxide (CO)

Carbon monoxide or just carbon oxide is a very poisonous gas for humans. The affinity between hemoglobin, which is a substance in blood responsible for oxygen absorption, and carbon monoxide is greater than between hemoglobin and oxygen [18]. This prevents hemoglobin to deliver oxygen to the body resulting in shortness of breathe. In addition it's an odorless and colorless gas making it almost impossible to discover without suitable equipment. As seen i Figure 1.2 Carbon monoxide is produced under conditions when the oxygen level is low and fuel fails to oxidize completely to carbon dioxide. Even during combustions when the oxygen concentration is high CO is always generated to some extent. This is because of incomplete combustions.

Hydrocarbons (HC)

A hydrocarbon is any chemical compound that consists only of the element carbon (C) and hydrogen (H). The simplest hydrocarbon is methane (CH_4) and only contains single bonds. Other types of bonds are also present, for example benzene (C_6H_6) which contains double bonds. Reduced hydrocarbons, like formaldehyde ($HCHO$) is often counted into this group. When exposed to hydrocarbons a normal reaction is usually to cough and choke but in extreme cases vomiting may occur. Hydrocarbons produces neurologic symptoms like drowsiness, poor coordination or even coma [18]. As seen in Figure 1.3 hydrocarbons are produced mainly during rich air-to-fuel mixtures (i.e $\lambda < 1$). In addition they are produced when the combustions is hindered by, for example, design faults in the combustion chamber. The reason for the increase when $\lambda > 1.15$ in the Figure is because the engine starts to misfire because of the very lean condition.

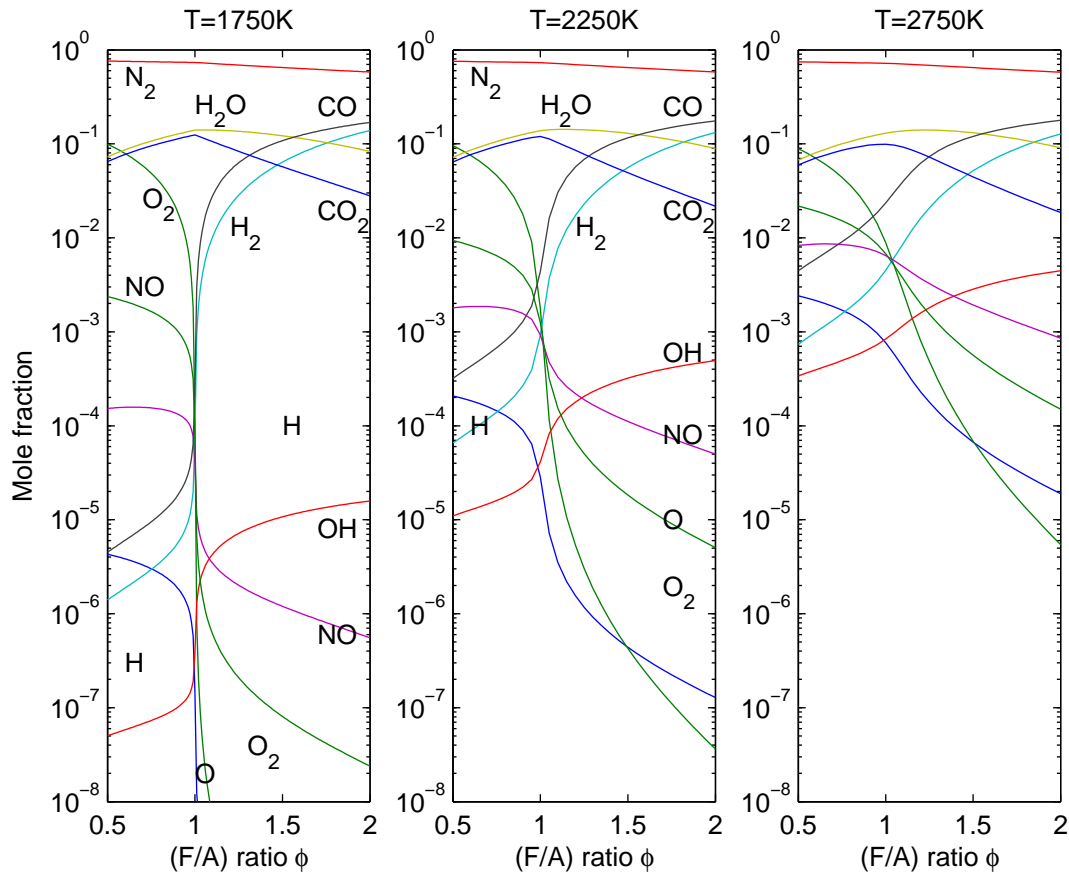


Figure 1.1: Species concentrations for varying mixture strengths. The three plots shows the results for different temperatures. Observe that gas concentrations is for different ϕ . (courtesy of Lars Eriksson [13])

Hydrogen (H_2)

Hydrogen is not a toxic gas but still very dangerous because it is very flammable. The gas is colorless, odorless and tasteless which makes it dangerous in a closed environment. Like carbon monoxide hydrogen is produced when $\lambda < 1$.

Nitrogen Oxides (NO_x)

When humans is exposed to nitrogen oxides it's believed that it aggravate asthmatic conditions. Furthermore NO_x doesn't dissolve very easy and it can therefore take time to notice warning signals of exposure. When NO_x is allowed to react with oxygen in the air it will produce ozone, which is an irritant. Ozone will eventually form nitric acid when dissolved in water. When dissolved in atmospheric moisture the result can be acid rain which damage both trees and entire forest ecosystems [18]. The concentration of NO_x is mainly dependent on the gas temperature in the engine, the temperature depends on many things, among others λ . In Figure 1.4 the (partially indirect) dependency of λ can be seen for the concentration of NO_x . The peak is at a slightly lean mixture.

1.4 Environmental Legislation

Already in the 50s some American towns had smog problems caused by Automobiles, therefore the US has traditionally been the leader when it comes to stringent limits for pollutants. This is specially true for the state of California which is know to have very stringent limits. Nowadays also Europe has stringent legislations, called

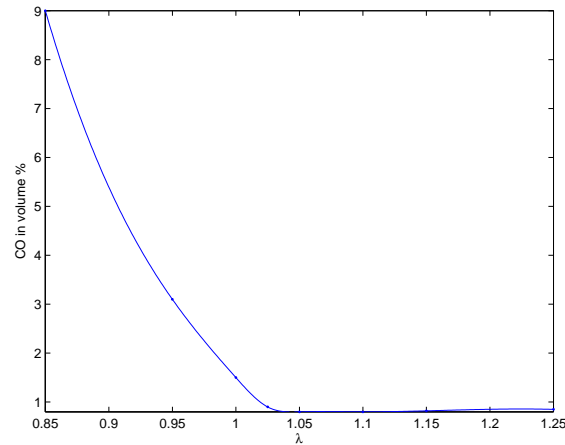


Figure 1.2: *CO* emissions from a gasoline engine. *CO* is produced when the oxygen level is low but never reaches a zero concentration even though $\lambda > 1$ because of incomplete combustion.

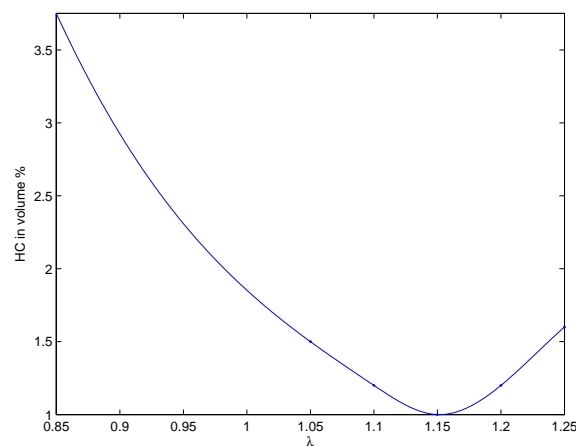


Figure 1.3: *HC* emissions from a gasoline engine. *HC* is produced when the oxygen level is low or when the combustion is hindered. In addition it can be produced when the engine is misfiring, this happens in the Figure at $\lambda > 1.15$

EURO X, where X stands for the version. The latest version of today (January 4, 2007) is EURO 4. In Table 1.1 different version and the introduction year is seen. To compare different cars under an emission standard a strict driving cycle is included into the standard. This scheme tells the tester exactly how to drive as well as ambient conditions, of course this is an indispensability for a correct and fair comparison. Every EURO emission standard has a slightly improved (i.e tougher) driving scheme and the latest ones incorporate cold-start conditions at -7°C . As seen in Table 1.2 the allowed emissions has very rapidly dropped, specially the latest one where it's roughly halved. The EURO standards is strictly speaking not just a standard for emissions but also includes demands for On-board diagnostics and durability of exhaust gas after-treatment systems. In addition limits for evaporative emissions, which is when gasoline evaporates directly from the tank, is included.

1.5 Progress

Today's cars have come a long way compared to cars manufactured before strict legislations were accepted. In these days computers are everywhere and a car is no exception, rather the opposite. According to TEEMA (Taiwan Electrical And Electronic Manufacturers Association) [14] the cost for the electronics in a car is today 20 percent of the total production cost but will in the next 10 years grow up to 50 percent. This computer explosion

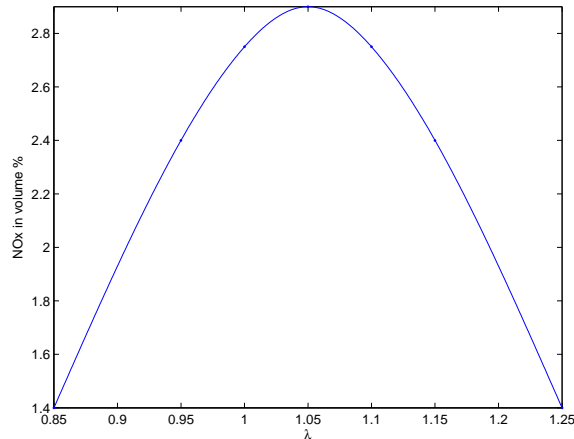


Figure 1.4: NO_x emissions from a gasoline engine. The NO_x is mainly dependent on temperature but also mixture strength influences. This is partially indirect through temperature. Observe that the peak is slightly displaced.

Emission standard	Introduction
EURO I	1992
EURO II	1996
EURO III	2000
EURO IV	2005
EURO V	Proposition to 2008

Table 1.1: Introduction years of Europeans emission standards [2]. The latest version today (EURO 4) has forced the car industry to significantly lower pollutants. EURO 5 (proposed 2008 for heavy duty vehicles) is believed to further increase the pressure on the industry.

has paved the way for more advanced control system for engines. Two of the major improvements for lowering emission the last 20 years are fuel injection and Catalytic Converters.

1.5.1 Fuel Injection

Prior to the 80s, nearly all engines used *carburetors* to mix air with fuel, simply speaking a mechanical device. After the 80s all cars used fuel-injection, with few words this is a computer powered ¹ technique used to get higher accuracy when measuring and mixing the gasoline/air-mixture.

1.5.2 Catalytic Converters

With the introduction of fuel injection new means to control pollutants produced by an engine became available. However no matter how the engine is controlled (more gasoline or less gasoline to same amount of air) you'll always end up with some undesired pollutant. If the engine is running rich more carbon-monoxide and hydrocarbons are discharged. On the other hand if the engine is running lean more NO_x discharged. What the car industry realized what that a device that restores the equilibrium was needed, an afterburner. This is what's called a Catalytic converter or a catalyst. Because a catalytic converter should restore equilibrium it works best at a very narrow band around the stoichiometric air-to-fuel ratio and this is where the computer powered fuel injection comes into place.

1.5.3 Lambda sensor

One of the most important sensor in today's cars, and the main topic for this thesis, is the lambda sensor (seen in Figure 1.5). It's job is to measure the amount of oxygen in the exhaust, the car's ECU will then use this infor-

¹Although in the beginning it existed fuel injection system powered by analog electronics and even mechanical solutions

Emission standard	HC + NO_x g/km	HC g/km	NO_x g/km	CO g/km
EURO I	0.97			2.72
EURO II	0.50			2.2
EURO III		0.2	0.15	2.3
EURO IV		0.1	0.08	1.0

Table 1.2: Limits for different emission standards [3]. The latest standard roughly halved the allowed emissions. The standard also includes on-board diagnostics, evaporative emissions and durability of exhaust gas after-treatment system.

mation to estimate if the fuel/air-mixture was right. This way the ECU gets a feedback of injected fuel and can avoid to only use pre-programmed values which doesn't take aging, ambient conditions etc into consideration. Without the lambda sensor, today's strict pollution regulations would be impossible to meet.



Figure 1.5: The Figure shows one of the most important sensor in a modern car, the lambda sensor. It was designed to sense the (A/F) -ratio so an effective feedback loop could be implemented in today's fuel injections. (courtesy of David Long [12])

1.6 Engine setup

All the tests will be performed on one of the department's engines, the L850. This motor is almost a standard engine from Saab except for the continuously dual independent variable cam timings. It's also connected to a PC running RTAI. This computer can take over parts of the engine-controller's work.

1.7 Reading Instructions

The thesis has a rather large prerequisites, this is for the convenience of readers with little or no knowledge on engines or Chemistry/Thermodynamics and could easily be skipped. Every section ends with a *conclusion*, this can easily be read alone if just interested in the results. Note that the last chapter summarize all important conclusions and makes corollary conclusions.

Chapter 2

Prerequisites

This chapter states some prerequisites needed to absorb the rest of the thesis. Every section starts with a small description of what it contains so the section safely can be skipped if the area already is grasped.

2.1 Engine

This section contains a small walk through of what kind of engines that exists today and what kind that will be used in this thesis. A small description of how an engine works is also given.

There exist many different types of engines today but the two most common in car industry is based on the diesel concept respective the Otto concept. The one based on the diesel concept often uses diesel as fuel and is therefore often called just a diesel engine. The other one, based on the Otto concept, has traditionally been using gasoline as fuel but nowadays it isn't unusual to run it on some other fuel like for example ethanol. The Otto concept was invented already in 1876 by the German scientist Nikolaus Otto [19]. The engine dealt with through out this thesis is a four-stroke reciprocating gasoline engine. This is the most common gasoline motor used in todays car industry. Of course other types is also used but in reality this is so seldom that a description would just confuse and is therefore not given.

2.1.1 Physical

An engine from a modern car is of course very complicated but the basic concepts can all be recognized from the prototype built by Nikolaus Otto. In Figure 2.1 the outline of a four-stroke engine can be seen. The piston is connected, via the rod, to the crankshaft. When the piston moves up and down the crankshaft begins to rotate. The inlet- and exhaust- valves are also shown. These controls the flow of fresh mixture and exhaust gas through the engine. The state when the piston is all the way down is called *Bottom Dead Center* and likewise the state when the piston is all the way up is called *Top Dead Center*.

2.1.2 Operation

The reason the engine is called a four-stroke engine is that the states (in this context called strokes) which the motor can be in is four. The strokes can be seen in Figure 2.2 and the flow are:

1. During the *induction stroke* (Figure 2.2a) the inlet valve is open and the piston is moving downwards. The result is that the engine is filled with fresh mixture through the inlet valve.
2. Next up is the *compression stroke*, which is seen in Figure 2.2b. The piston has turned direction and is now moving upwards. Both the valves is closed and the newly inducted fresh mixture is compressed.
3. The *power stroke* starts with a spark from the spark plug (seen in Figure 2.2c) which ignites the mixture. The piston is therefore forced downwards by the expanding gases. It's not a regular explosion but rather a controlled burning of the gases. This stroke is the only stroke that produces power, the other ones consume.
4. The last stroke, seen in Figure 2.2, is the *exhaust stroke*. The piston has once again turned direction and is moving upwards and the exhaust valve has opened. The piston therefore forces the newly burned gases out through the exhaust and a new induction stroke can start.

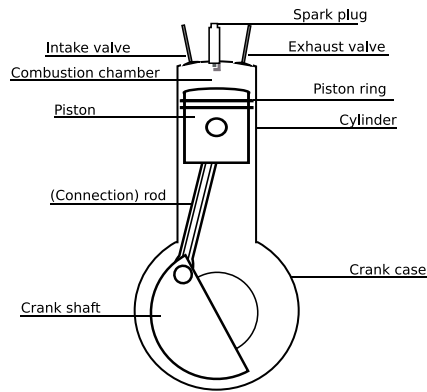


Figure 2.1: An overview of a modern engine, all the basic concepts are recognized from the prototype built by Nikolaus Otto. The piston moves up and down making the crankshaft rotate. This in turns makes (through the gearbox etc) the wheel turns.

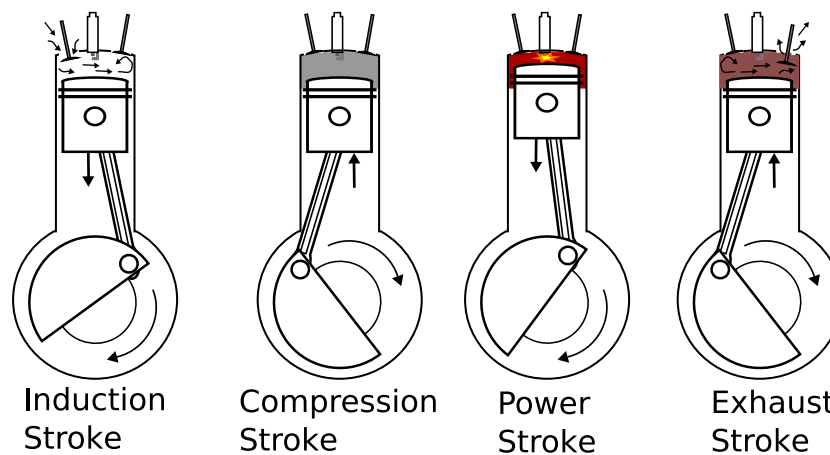


Figure 2.2: The operation of a four-stroke engine. Each picture symbols a stroke. During the Induction stroke fresh mixture is drawn in, which later is compressed during the compression stroke. The power stroke ignites the compressed mixture and produces rotation energy. Finally the burnt gases is exhaled during the exhaust stroke.

In nature nothing happens instantly and this of course also the case in an engine. The result is that the valves can not open and close at there exact stroke. For example the exhaust valve opens some time before the piston has reached BDC. Even the spark from the spark plug actually come sometime before the piston is in TDC.

2.1.3 Intake

An engine needs both air (oxygen) and fuel (gasoline) to function properly. A modern car has fuel injection, see Section 1.5.1, which means that the fuel is injected with one or several injectors. An injector is an electrical controllable valve which work under high pressure. The amount of fuel injected is controlled by the engines ECU. The amount of air on the other hand is normally, either direct or indirect through the ECU, controlled by the driver and the accelerator. In the end another kind of valve called a throttle is used to control the amount of air actually inducted. The injector and throttle can be seen in Figure 2.3.

2.1.4 Turbo

A modern car often incorporates a turbo to boost efficiency. The turbo can be divided into two parts: The turbine and the compressor. After the exhaust valve of the engine the turbine part of the turbo is located, this part starts

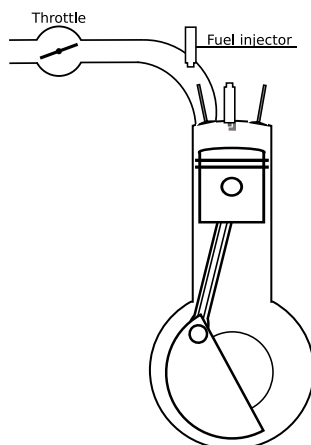


Figure 2.3: The intake side of a modern engine. The fuel is injected through one or several fuel injectors, which can be seen in the Figure. The amount of air entering the engine is controlled through a valve called throttle, this is seen in the top left.

to spin from the movement of the exhaust gas. The turbine is in turn directly connected to the compressor part which compresses air entering the engine. This way more air can enter the engine resulting in more power.

2.2 Chemistry

The text in this chapter is actually from upper secondary class (in Sweden *gymnasieskola*) and is easily skipped if already grasped.

2.2.1 Chemical equilibrium

Chemical equilibrium is the state when a reaction and its reverse reaction occurs at the same rate. That is, the concentrations of the participating gases remains constant over time. It should be noted that although that the concentrations remains, the reaction (and its counter reaction) continues. The concentrations of the participants in a reaction under chemical equilibrium is related to each other by

$$K = \frac{[C]^n [D]^p}{[A]^k [B]^m} \quad (2.1)$$

where K is the equilibrium constant. An example is the water-gas equilibrium which is the collaboration between carbon oxide, water, hydrogen and carbon dioxide, these reactions is described by $K = \frac{[CO][H_2O]}{[CO_2][H_2]^m}$ where K is the Water gas equilibrium constant. The reaction rate is highly dependent on temperature, if the temperature drops to low the reaction is sad to be frozen and almost no reactions occurs. For the water gas equilibrium this happens at approximately 950K. However in presence of a catalytic substance the reactions can occur at much lower temperatures.

2.3 Thermodynamics

When steam powered engines conquered the world the need for a physics to optimize these engines developed. The result was thermodynamics, a branch of physics that deals with temperature, pressure and volume. A system in thermodynamic is viewed at at macroscopic level but the prediction of the system is made through statistical views at particle level. This chapter states the important thermodynamics [6] for this thesis.

1. **Boltzmann factor** - The relative probability for a system to be in thermodynamic equilibrium is called the Boltzmann factor. At temperature T it's expressed as:

$$e^{-\frac{E}{K_b T}} \quad (2.2)$$

Where K_b is the Boltzmann constant and E is the systems energy.

2. **Chemical potential** μ_c - Chemical potential is, the name in spite, a thermodynamic term. If you hold entropy and volume constant the chemical potential of a system is how much the energy will change if new particles is added.
3. **Entropy** - A systems temperature, pressure and density can differ over space but over time they all tend to equalize. For example open and turn off the fridge and soon the temperature has equalized between the room and the fridge. Entropy is a measure of how "equalized" a system is.
4. **Mechanical equilibrium** - When the sum of the forces and moments on each particle of a system is zero the system is said to be in mechanical equilibrium.
5. **Thermal equilibrium** - For a system to be in thermal equilibrium it's temperature should be constant in time and space.
6. **Thermodynamic equilibrium** - A system is said to be in thermodynamic equilibrium if the system is in chemical-, mechanical- and thermal-equilibrium. If a system is present in this state all visible observables is unchanged over time and space.

2.4 Electro chemistry

This chapter describes the electro chemistry needed for this thesis.

1. **Galvanic cell** - This cell, named after a Italian physicist who lived in the 18th century, consisted of two metal plates with a electrolyte connection between them.

Chapter 3

Lambda sensors

So far only the basics about the lambda sensors has been covered (see 1.5.3), this chapter goes into detail of the design and structure of different kinds of lambda sensors.

Common for all lambda sensors is that they try, in some way or another, measure the amount of oxygen in the exhaust. This way the engine controller can estimate the actual A/F-ratio and thereby reduce emissions. Often two sensors are used on a modern engine, the main sensor is located in the exhaust manifold (after the turbo if one exists) and before the catalytic converter. The second one is located after the converter. The placement is seen in Figure 3.1. With a second sensor downstream of the catalytic converter, the controller can diagnose the converter and even give an estimate of the oxygen level. There are basically two types of lambda sensors, the switch type (also called narrow band, ego or discrete type) and the wide band type (also called uego).

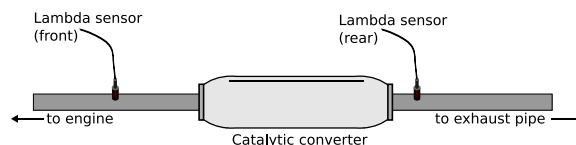


Figure 3.1: On a modern car two lambda sensors is often used, one before the converter and one after. The sensor located before the converter is the main one, responsible for the mixture strength measuring. The second one is used for diagnose.

3.1 Switch type

The switch type lambda sensor has been the most common over the years since fuel injection was first utilized. Recently it has been replaced as the main sensor but is still the most common choice as second sensor (after the catalyst). This sensor has an highly non-linear output with very rapid change at the stoichiometric A/F ratio seen in Figure 3.2. Because of the non-linear output this sensor is not reliable to measure the actual A/F-ratio. Instead it's used as a boolean value or an on/off-switch. Everything below $\lambda = 1$ is regarded rich and everything over is lean. Because of the relay characteristic of this sensor together with a time delay a oscillating behavior of the resulting lambda (see Figure 3.3) is unavoidable. Two different kinds of techniques can be discerned for switch type sensors, the zirconia sensor and the titania sensor. Of the two the zirconia variant is the far most common among car manufacturers and this is also the one mainly dealt with throughout this thesis.

3.1.1 Physical structure

Most switch type sensors are today of planar type, meaning that they consist of layers on top of each other [4]. One of the sensor's outer layer is exposed to the gas to measure. The other outer layer is exposed to a reference gas. In the case when using a lambda sensor in a car the gas to measure is exhaust fumes and the reference is air.

First of all the sensor is placed in a housing, its main purpose is to protect the sensitive sensor from small particles in the exhaust. In addition the heat transfer from the sensor is reduced. The housing is made of metal and is usually in shape of a cylinder. To allow the gas to pass inside to the actual sensor the housing has small

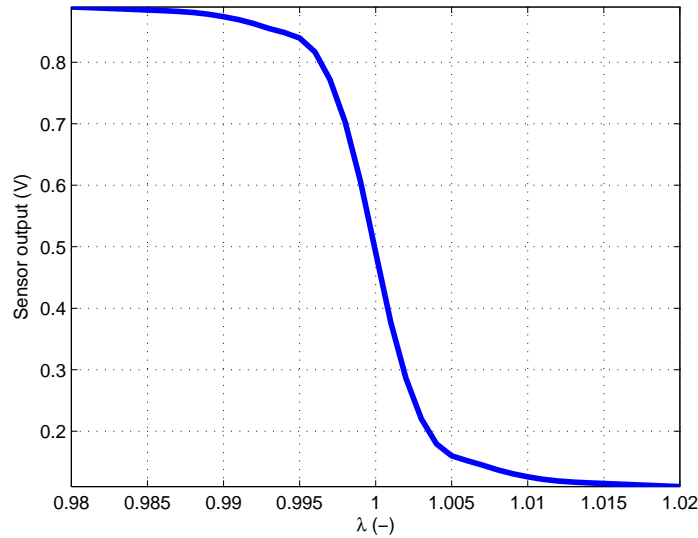


Figure 3.2: Typical output from a switch type λ -sensor. The highly non-linear output seen makes this sensor unsuitable for an measure of the exact A/F-ratio. Instead it's used as a boolean value or an on/off-switch.

holes. As seen in Figure 3.4 the first layer (leftmost in the Figure) of the actual sensor is the protection layer which protects the sensor from direct gas exposure. The gas diffuses through the protection layer on to the next layer. It's therefore important that the protection layer is porous and allows the exhaust gases to pass through freely. The layer is always of ceramic, the type may vary. The next layer is one of the electrodes, specifically the cathode. The electrodes are catalytic and mainly made of platinum but may have other catalytic additives. This helps the exhaust gas into chemical equilibrium which is needed for a reliable measure. In the middle of the sensor is the electrolyte layer, this is where the actual voltage between the anode and cathode is created. The electrolyte is Zirconia (ZrO_2) with additives to enhance oxygen ions for the Zirconia sensor or Titania TiO_2 for the Titania sensor. The reference side is built accordingly, however it often lacks protection layer because its environment is not so hostile. Moreover, as the output from the sensor is highly temperature dependent (for further information see next section) the sensor often incorporate a heater. This way the sensor's temperature can be controlled for a better output.

3.1.2 Zirconia sensor

This sensor produces a voltage difference between the anode and cathode in the electrolyte. As for the function of the unit it's forming a galvanic cell, a good way to describe a galvanic cell is through the nernst equation. The voltage level from the sensor is high when oxygen level is low, so in reality the absence of oxygen is measured.

Function

The exhaust gas diffuses through the protection tube and the protection layer onto the electrodes where they react with each other and end up close to chemical equilibrium. Also the protection layer helps to achieve this as it acts like a diffusion barrier. When oxygen is adsorbed on the electrode a concentration difference arises between the electrode and the oxygen ions in the electrolyte. The ions in the electrolyte feels a strong attraction from the electrode and are drawn towards it. The ions donates two electrons to the electrode and a voltage difference arises. Of course the other way around is also possible when ions take electrons from the electrode.



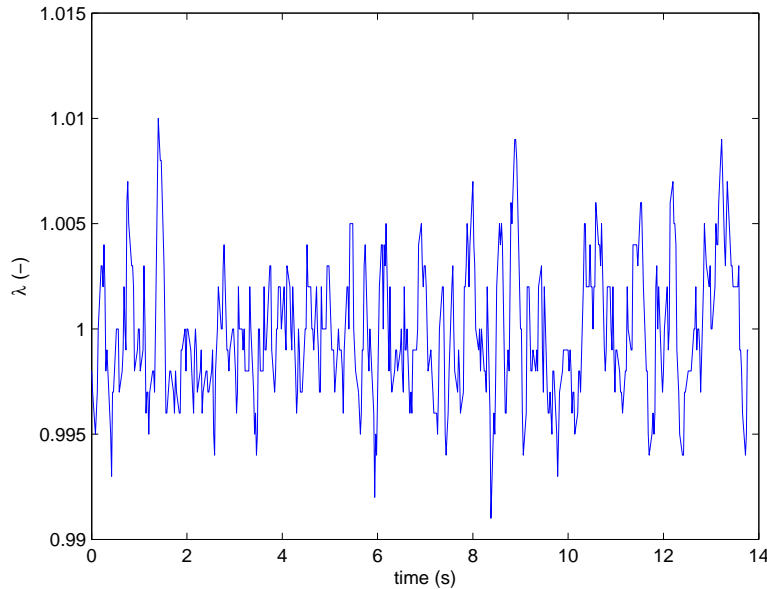


Figure 3.3: The Figure shows the resulting lambda when using a switch type λ -sensor as feedback to the ECU. The oscillating behaviour comes from limited information that can be used from this kind of sensor, the mixture is seen either as rich or as lean and nothing in between.

So far only oxygen is taking part in the operation but additionally the oxygen ions react directly with the reducing species (mainly H_2 and CO because of their high concentration but also HC) donating additionally electrons. The donated electrons and their holes in the ion grid build up an electronic field which obstruct the electron exchange until the system reaches a chemical equilibrium. Meanwhile the same process is active at the reference side building up a voltage difference between the cathode and the anode. This is the actual voltage measured to get a reading from the sensor.

3.1.3 Titania sensor

Unlike the Zirconia sensor this type doesn't produce its own voltage but has a resistive output. Otherwise the function is the same. The controller feeds the sensor with a low current supply and measures the actual voltage drop across the sensor. The resistance varies from a couple of $k\Omega$ for a rich mixture to ten times more for a lean mixture. This sensor is much faster than the zirconia sensor but on the other hand it's more expensive. Car industry has come to favor the slower but cheaper variant. The reason is that the titania sensor is in the same price range as the much better wide band sensor.

3.1.4 Evaluation of sensor

To evaluate the functions of the discrete lambda types the nernst cell equation is here given without proof. For more details see Section 4.2.1.

$$E = E^0 + \frac{kT}{e} * \ln \frac{[Ox]}{[Red]} \quad (3.3)$$

Where E^0 = Potential of the cell at standard conditions and $\frac{[Ox]}{[Red]}$ = The ration between oxidizing and reducing molecules. The unit has a linear temperature dependence as seen in the equation, this is why a heater is always included in new sensors. Without the heater the sensor would have to rely on exhaust temperature to get warm during a startup. In addition the temperature is more stable with a heater, which is a good thing for example during an overtake. When the accelerator is pressed the engine deliverers more power and thereby increasing the exhaust temperature. Although the heater nowadays is mandatory the gain error doesn't completely disappear. This is because the temperature in the nernst equation isn't the surrounding temperature alone but rather a function of

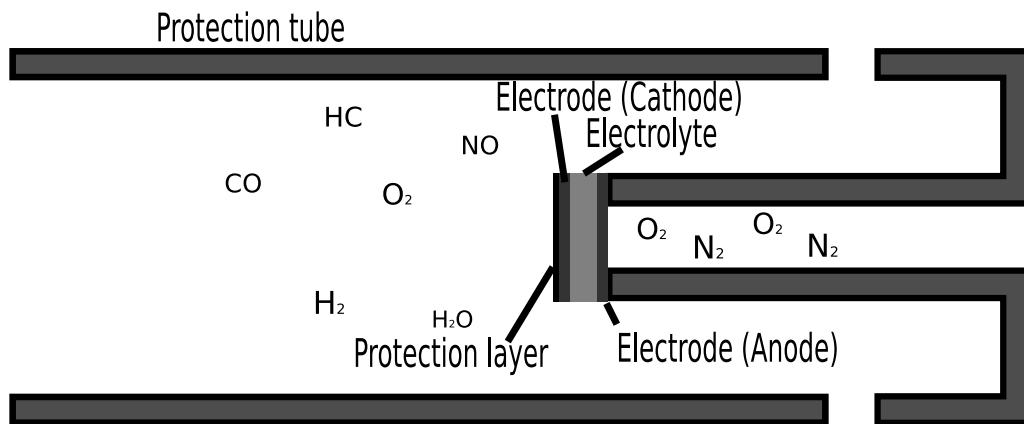


Figure 3.4: The physical structure of a planar switch type λ -sensor. This is the structure used by all modern λ -sensors.

all participating molecules, which includes the gas temperature, i.e. even though the unit itself always has the same temperature the reacting gases doesn't and thus creates a gain error. However, the gain error isn't important for normal operation with this kind of sensor. This is because the sensor will produce a switch characteristic voltage output with a large difference between the 'low' and 'high' value. So when a gain error do occur the actual switch characteristic doesn't change much as seen in Figure 3.5. It's easy to use the information to find out if the engine is running rich or lean but all other information is uncertain.

3.2 Wide band

One of the latest big innovations for reducing emissions is the wide band lambda sensor. Although it has existed for several years it's not until recent years that it has been used in production by the car industry. Unlike the switch type this sensor misses the relay characteristics, this is seen in Figure 3.6. The output is not fully linear but it's possible to estimate the degree of a lean or a rich mixture with high accuracy. For example a Bosch sensor has a measurable λ -range of around 0.7 – 4 [4]. With a wide band sensor a whole new set of control strategies can be utilized. In addition the oscillating control behavior found with the switch type sensor can be avoided.

3.2.1 Physical structure

The structure is much like two switch type zirconia sensors connected in series with a cavity in between. The structure is shown in Figure 3.7.

3.2.2 Function

The inner switch type sensor is functioning like normal and measures the oxygen level in the cavity. The outer sensor is working in the opposite direction and, instead of giving a voltage, a current is applied and the sensor pumps oxygen in or out from the cavity. Gas enters the cavity through diffusion, two sorts of diffusion can be sorted out in this case: Molecular and Knudsen. The rate of transport in molecular diffusion is governed by the diffusivity and the concentration gradient. Where as Knudsen diffusion also is governed by temperature [5]. This type of sensor is always bundled with a controller, the goal of the controller is to create equilibrium in the cavity. To do so the controller looks at the output from the nernst cell and pumps in (or out) just enough oxygen to give equilibrium. The amount of current used in the oxygen pump is proportional to the mixture strength. As the sensor is highly temperature dependent and it misses the redundancy in the output from the switch type sensor

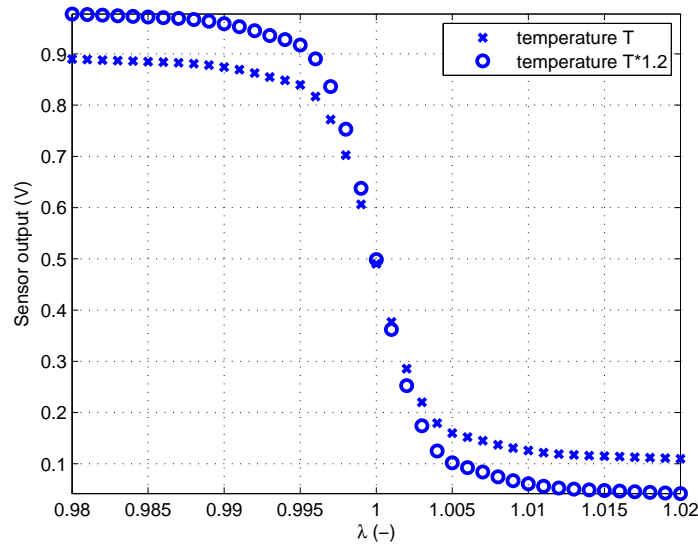


Figure 3.5: The principle output from the same discrete λ -sensor but with different temperatures. As seen the useful information (rich or lean) isn't ruined when changing temperature.

(see Section 3.1.4) the controller needs to incorporate a much better temperature controller. To be able to control the temperature carefully a feedback is needed, this is cleverly done by measuring the resistance in the Nernst cell. Many solutions are possible but perhaps the smartest (no analog switches is needed and no need for turning off the pump circuit) is to apply a high-frequency signal to the nernst cell. By doing so the resistance can be measured (by AC-coupling the high-frequency signal) and this can be done in real time without turning of the rest of the sensor.

3.2.3 Evaluation of sensor

Unlike the switch type sensor, this sensor needs a external controller. Also, as with all controllers, there are hundreds of different control strategies to choose from. This means that although two system share the same sensor type, two different controllers (or just two different control strategies) may be used, differentiating the systems completely. The sensor is also more sensitive for surrounding factors, those must either be controlled or at least be compensated for by the controller. The wide band sensor enable linear closed loop control, not just to $\lambda = 1$ but also for other λ . Diesel engines, heavy-duty trucks, compressed natural gas (CNG) and other engines not running at stoichiometric mixture can gain much in implementing a wide band sensor into the ECU [16].

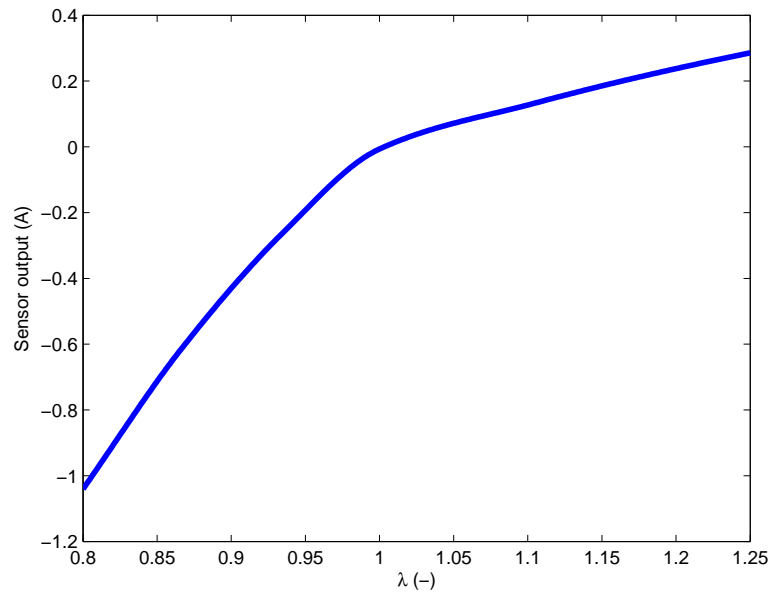


Figure 3.6: Typical output from a wide band λ -sensor. The output is almost (piecewise) linear.

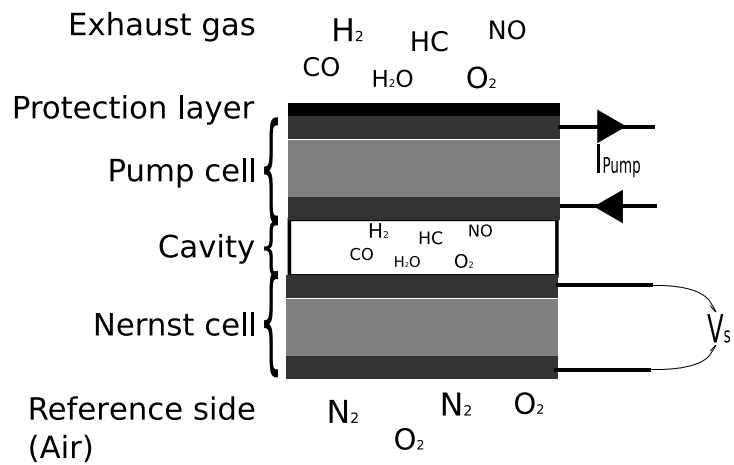


Figure 3.7: Physical structure of a wide band sensor. The structure is in fact two switch type zirconia sensors connected in series with a cavity in between.

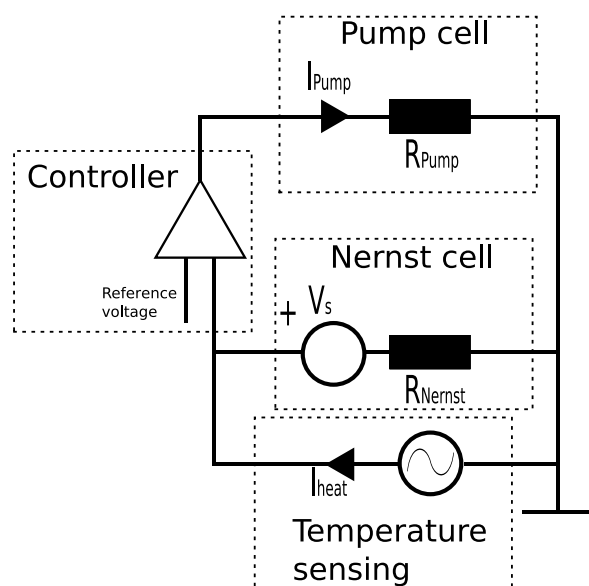


Figure 3.8: Electrical structure of a wide band λ -sensor. The circuit is divided into four parts. The pump- and nernst-cell are the actual sensor where as the controller- and the temperature sensing-block is in the controller.

Chapter 4

UEGO Model

Common for all the types of lambda sensors is that they try to measure A/F ratio through measuring the amount of oxygen in the exhaust. Although this seems like a simple idea at first it's not that easy. First of all the way from measured oxygen level to A/F ratio isn't straightforward. The mixture may not be in complete equilibrium, for example the water-gas shift reaction may be unbalanced. Secondly the uego sensor is very sensitive to changes in surrounding parameters.

To do calculations of, for example, temperature sensitivity a model in Matlab/Simulink is developed. In this chapter an evaluation of models is given, the next chapter holds the actual results using the final model. The model is divided in to three parts, *switch type*, *diffusion* and the *oxygen pump*. In addition the use of a controller is needed for getting an output from the UEGO. In reality processing of the signals is needed between the parts. All model parameters calculated in this chapter can be found in Appendix B.

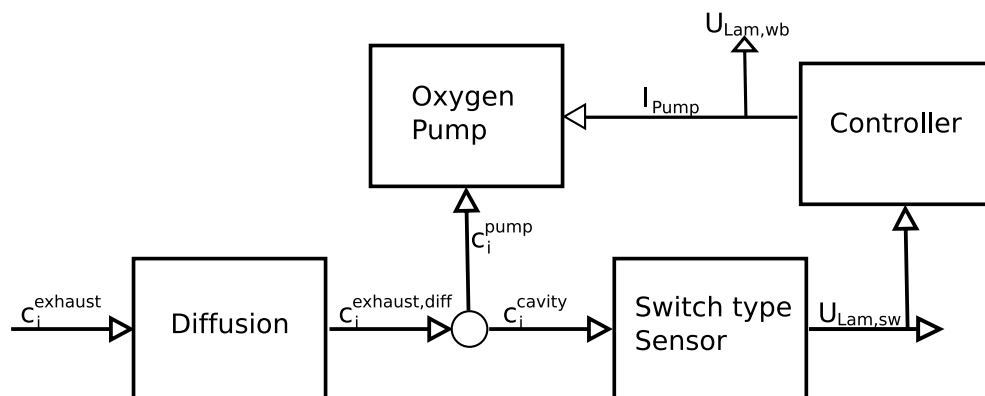


Figure 4.1: Wide band model overview. The model is divided into three parts plus the controller part. In reality signal processing between them is also needed.

4.1 Data

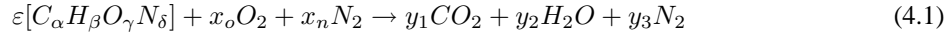
The data available to test models and conclusions have been sparse. The only available data was from [15]. More about the data in Appendix A.

4.1.1 Exhaust model

Since the supply of data has been inadequate a model for exhaust components has been developed from [3] [5], the result is very similar to Heywood [8]. The real data is of course irreplaceable but an exhaust model is a perfect complement as test cases can easily be created.

The balance equation (4.1) describes the reaction between air and a general one-substance fuel. Air is assumed to consist of oxygen and non-participating substances, where the non-participating substances all are

assumed to be nitrogen. Therefore $x_o + x_n = 1$ applies where x_o is the fraction oxygen and x_n is the fraction of nitrogen.



Consequently the constraint equations becomes:

$$\text{Carbon} : \varepsilon\alpha = y_1 \quad (4.2)$$

$$\text{Hydrogen} : \varepsilon\beta = 2y_2 \quad (4.3)$$

$$\text{Nitrogen} : \varepsilon\delta + 2x_n = 2y_3 \quad (4.4)$$

$$\text{Oxygen} : \varepsilon\gamma + 2x_o = 2y_1 + y_2 \quad (4.5)$$

This is a normal linear equation system, with $x_n = 0.79$ and $x_o = 0.21$ the solution becomes:

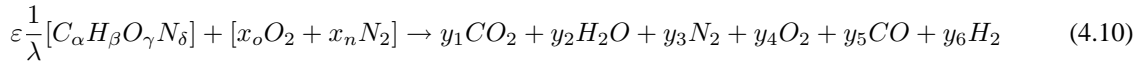
$$y_1 = \frac{0.21\alpha}{\alpha + 0.25\beta - 0.5\gamma} \quad (4.6)$$

$$y_2 = \frac{0.105\alpha}{\alpha + 0.25\beta - 0.5\gamma} \quad (4.7)$$

$$y_3 = \frac{0.79 + 0.105\delta}{\alpha + 0.25\beta - 0.5\gamma} \quad (4.8)$$

$$\varepsilon = \frac{0.21}{\alpha + 0.25\beta - 0.5\gamma} \quad (4.9)$$

This equation is only valid for complete combustion, which in reality never happens. For the lambda sensor model the lack of H_2 and CO is the biggest drawback. To extend the model CO and H_2 is added in the equation. In addition the ability to run lean or rich is added by introducing λ into the equation, this also requires O_2 in the exhaust gas when the engine is running lean, see equation (4.10).



For simplicity CO and H_2 are regarded zero when running lean, likewise is O_2 when running rich. When running rich the water-gas shift reaction is assumed to be correct, see equation (2.2.1). The constraint equations is different dependent on the mixture strength: **Lean**

$$\text{Carbon} : \varepsilon \frac{1}{\lambda} \alpha = y_1 \quad (4.11)$$

$$\text{Hydrogen} : \varepsilon \frac{1}{\lambda} \beta = 2y_2 \quad (4.12)$$

$$\text{Nitrogen} : \varepsilon \frac{1}{\lambda} \delta + 0.79 * 2 = y_3 \quad (4.13)$$

$$\text{Oxygen} : \varepsilon \frac{1}{\lambda} \gamma + 0.21 * 2 = 2y_1 + y_2 + 2y_4 \quad (4.14)$$

Rich

$$\text{Carbon} : \varepsilon \frac{1}{\lambda} \alpha = y_1 + y_5 \quad (4.15)$$

$$\text{Hydrogen} : \varepsilon \frac{1}{\lambda} \beta = 2y_2 + 2y_6 \quad (4.16)$$

$$\text{Nitrogen} : \varepsilon \frac{1}{\lambda} \delta + 0.79 * 2 = y_3 \quad (4.17)$$

$$\text{Oxygen} : \varepsilon \frac{1}{\lambda} \gamma + 0.21 * 2 = 2y_1 + y_2 + y_5 \quad (4.18)$$

The solution is seen in Table 4.1. This yields a complexer solution than before but still manageable. As seen the equations result in a non-differentiable function at $\lambda = 1$, this could mean problems with discontinues in some cases.

Specie	$\lambda > 1$	$\lambda < 1$
CO_2	$\alpha \frac{1}{\lambda} \varepsilon$	$\alpha \frac{1}{\lambda} \varepsilon - y_5$
H_2O	$\beta \frac{1}{2\lambda} \varepsilon$	$0.42 - \frac{1}{2\lambda} \varepsilon (2\alpha - \gamma) + y_5$
N_2	$0.79 + 0.5\delta \frac{1}{\lambda} \varepsilon$	$0.79 + 0.5\delta \frac{1}{\lambda} \varepsilon$
O_2	$0.21(1 - \frac{1}{\lambda})$	0
CO	0	y_5
H_2	0	$0.42(\frac{1}{\lambda} - 1) - y_5$

Table 4.1: The resulting gas concentration under equilibrium using linear equations. The equations is continues at $\lambda = 1$ but not differentiable, this could produce discontinues later on.

$$y_5 = \frac{-b + \sqrt{b^2 - 4ac}}{2a}$$

$$a = 1.0 - K_p$$

$$b = 0.42 - \frac{1}{\lambda} \varepsilon (2\alpha - \gamma) + K_p (0.42(\frac{1}{\lambda} - 1) + \alpha \frac{1}{\lambda} \varepsilon)$$

$$c = -0.42\alpha \frac{1}{\lambda} \varepsilon (\frac{1}{\lambda} - 1) K_p$$

The model could be extended to NO_X and HC but this is not necessary as the implemented lambda sensor model does not use these concentrations.

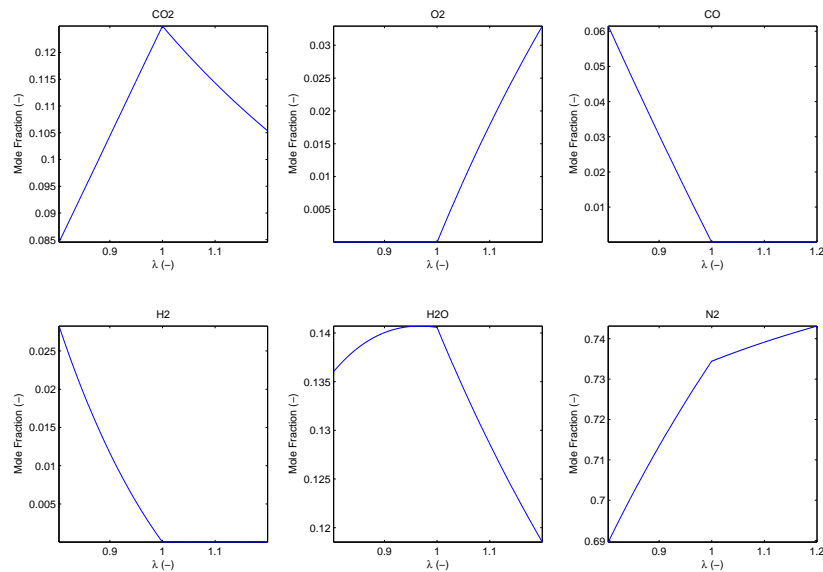


Figure 4.2: Output from exhaust gas model. The functions are clearly linear and non-differentiable at $\lambda = 1$.

4.2 Switch type model

One of the parts building up a wide band sensor is, as stated in Section 3.2, a switch type sensor. Therefore a good model for a switch type sensor has to be developed. The pump model will use this model to know which way to pump oxygen, the most important part to get right is therefore the switch characteristics. The previous chapter also states that the switch type lambda sensors can be described with the nernst equation.

4.2.1 Nernst equation

In 1920 Walther H. Nernst received the Nobel prize for “in recognition of his work in thermo chemistry”, his work led to the Nernst equation which correlates the chemical energy and the electric potential of a galvanic cell. The equation can be written as:

$$E = E^0 + \frac{kT}{e} * \ln \frac{[Ox]}{[Red]} \quad (4.19)$$

E^0 = Potential of the cell at standard conditions and $\frac{[Ox]}{[Red]}$ = The ration between oxidizing and reducing molecules. The equation is most easily derived from chemical potential and the Boltzmann factor. As the Boltzmann factor is a relative probability the ratio between the oxidized and reduced molecules is good starting-point. This ratio is elementary the probability for a molecule to be oxidized over to be reduced. So the Boltzmann’s factor gives:

$$\frac{[Ox]}{[Red]} = \frac{e^{-\frac{E_{ox}}{K_b T}}}{e^{-\frac{E_{red}}{K_b T}}} = e^{\frac{E_{red} - E_{ox}}{K_b T}} \quad (4.20)$$

Where E_{red} and E_{ox} are the energy barriers needed to be overcome for a electron to switch owner. The chemical potential μ_c has for this system the solution of $E_{red} - E_{ox}$ when considering that the entropy and volume should be constant. The natural logarithm on both sides becomes:

$$\ln \frac{[Ox]}{[Red]} = \frac{\mu_c}{K_b T} \Rightarrow \mu_c = K_B T \ln \frac{[Ox]}{[Red]} \quad (4.21)$$

To get electrical potentials instead of chemical, the equation is divided with e (as it is electrons that changes owner).

$$E = \frac{K_B T}{e} \ln \frac{[Ox]}{[Red]} \quad (4.22)$$

Even though $\frac{[Ox]}{[Red]} = 1$ there can be a voltage over the electrodes, therefore an offset E^0 is added, and equation (4.19) is finally received.

4.2.2 Linear Regression models

As starting point for all linear approximations of the switch cell, equation (4.19) is used. These models try to linearize the equation so they can be solved by a least square method.

Oxygen based model 1

A switch type sensor is often called an oxygen sensor, although not the whole truth (compare to equation (4.19)) there is an oxygen dependency. As seen in Figure 4.3 the sensor follows the oxygen concentration quite well, at least on the lean side. In this case, the switch characteristics is the most important part. This causes the oxygen based model where only the oxygen concentration is used. The equation (4.19) is used and a least square method is applied to get a reasonable value on $\frac{[Ox]}{[Red]}$. Although in reality the equation involve fractions of the electrode occupied with substances, it seems reasonable to simplify this with the gas concentration level. At least the occupancies of the electrode clearly must be highly dependent of the concentration level. As the oxygen concentration is inverted compared to the voltage from the sensor the formula $1 - E$ is fitted.

$$\begin{aligned} 1 - E &= 1 - E^0 + \frac{kT}{e} * \log \frac{[Ox]}{[Red]} \\ &\approx k_0 + \frac{kT}{e} * \log k_1 * [O_2] \\ &\approx \text{/taylor around the midpoint } m/ \\ &\approx k_0 + \frac{kT}{e} * (\log(k_1 * m) + [\frac{d}{dx} \ln(k_1 * x)]_{x=m} * ([O_2] - m) + ..) \\ &\approx k_2 + k_3 * [O_2] + k_4 * [O_2]^2 \end{aligned}$$

For some k_2 , k_3 and k_4 . The result can be seen in Figure 4.4. The model has rather poor resemblance, specially on the rich side. The saturated behavior on this side is probably a consequence of the very low concentration of oxygen. The lean side is rather noisy, most certainly a consequence from using both the rich and the lean side for the least square. This results in a very high sensitivity for oxygen.

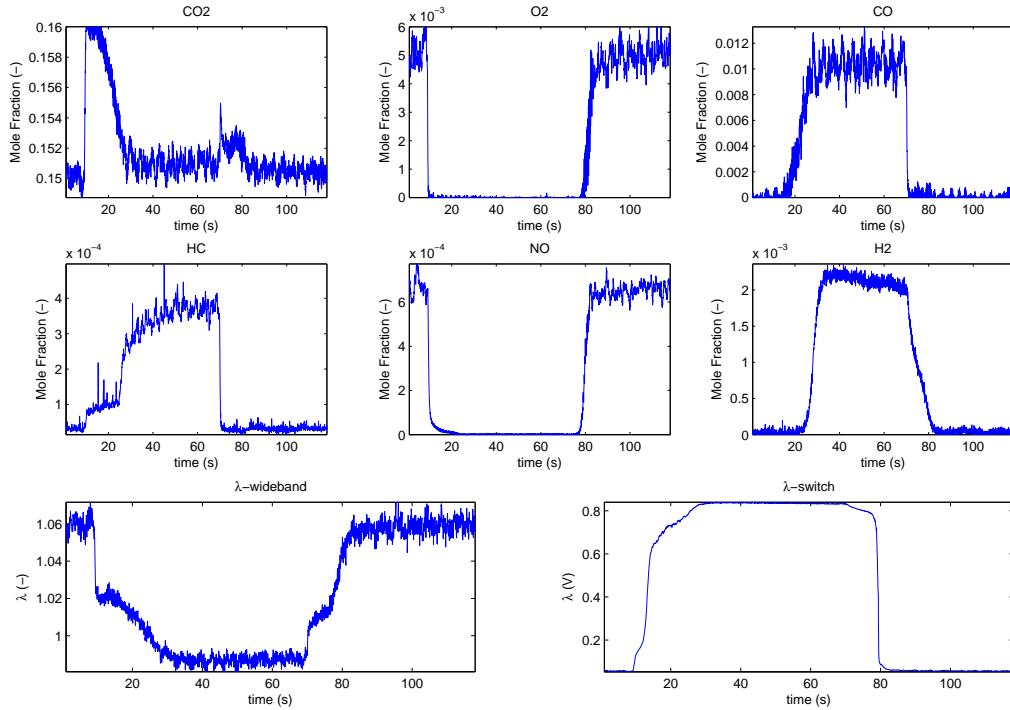


Figure 4.3: Gas concentrations for first set of test data. For more data see Appendix A. For the model only CO, H_2 and O_2 is used but in reality all the gases has more or less an effect on the sensor.

Oxygen based model 2

The second oxygen based model is based on the fact that on the lean side the sensor must be oxygen driven as no other gases are present. This model uses the same approximation of the nernst equation as the first oxygen based model but differ on the approximation interval. Instead of looking at the whole interval when using the least square algorithm only the lean part is used. Figure 4.5 displays the result. As expected the model shows great resemblance on the lean side but poor on the rich. As only the lean side is used for the least square the high sensitivity from Oxygen based model 1 is gone. This makes the noisy behavior disappear but also causes the model to have too low swing at the rich side.

Extended gas model

This model uses the same approach as the two preceding but instead of doing an approximation using only oxygen the model is extended with more gases. Carbon oxide and hydrogen are two strongly reducing gases and the concentrations of these two are fairly agreeable with the sensor output on the rich side.

$$\begin{aligned}
 E &= E^0 + \frac{kT}{e} * \log \frac{[Ox]}{[Red]} \approx k_0 + \frac{kT}{e} * \log \frac{k_1 * [O_2] + k_2}{k_3[CO] + k_4[H_2] + k_5} \\
 \Rightarrow e^{\frac{E * e}{kT}} &= e^{\frac{k_0 e}{kT}} * \left(\frac{k_1 * [O_2] + k_2}{k_3[CO] + k_4[H_2] + k_5} \right) = \frac{k_{1'}[O_2] + k_{2'}}{k_3[CO] * k_4[H_2] + k_5} \\
 \Rightarrow e^{\frac{E * e}{kT}} * k_5 &= k_{1'}[O_2] + k_{2'} - e^{\frac{E * e}{kT}} * (k_3[CO] + k_4[H_2]) \\
 \Rightarrow e^{\frac{E * e}{kT}} &= k_{1''}[O_2] + k_{2''} - e^{\frac{E * e}{kT}} * (k_{3'}[CO] + k_{4'}[H_2])
 \end{aligned}$$

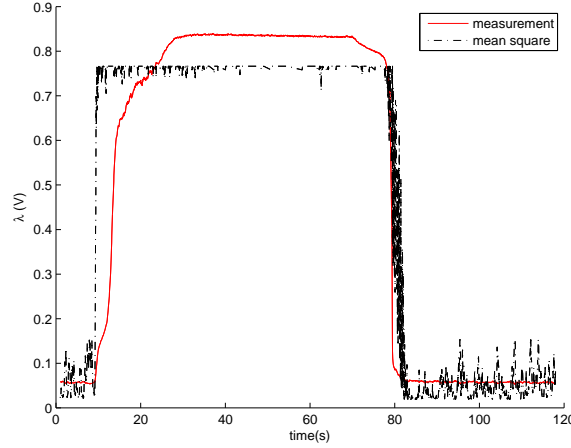


Figure 4.4: The Figure shows the first Oxygen based model versus the measure. The model has rather poor resemblance, saturated on the rich side and noisy on the lean.

For some $k_{1'}$, $k_{2'}$, $k_{3'}$ and $k_{4'}$. This looks like an ordinary least square but unfortunately this generates a badly conditioned matrix. So instead a Taylor expansion like in the previous section is used.

$$\begin{aligned}
 E &= 1 - E^0 + \frac{kT}{e} * \log \frac{[Ox]}{[Red]} \\
 &\approx k_0 + \frac{kT}{e} * \log \frac{k_1 * [O_2]}{k_2 [H_2][CO]} \\
 &\approx \text{/taylor around midpoints /} \\
 &\approx k_{0'} - k_{1'} * [O_2] + k_{2'} * [CO] + k_{3'} [H_2]
 \end{aligned}$$

For some $k_{0'}$, $k_{1'}$, $k_{2'}$ and $k_{3'}$. The result is displayed in Figure 4.6. As seen the model has the same deficiency as the Oxygen based method 1. As both the lean and the rich areas of the information are used for the least square the sensitivity for O_2 gets too high on the lean side and likewise for CO and H_2 on the rich side.

4.2.3 Full Auckenthaler

In [3] by Auckenthaler a model for a switch-type sensor is described, the model is divided in to three parts; diffusion, electrode and electrolyte. The model is briefly described here for convenience.

Protection Layer

This part accounts for all the diffusion phenomenas. The concentrations $c_i^{electrode}$ are calculated mainly from $c_i^{exhaust}$ and the mass transfer rate \dot{m}_i between the electrode and the gas phase due to sorption¹. This part was never implemented due to the decision not to use this model, more on this in Section 4.2.5.

Electrode

Here the occupancies on the electrode, θ_i , is calculated from the concentrations after the protection layer. This is done by using Langmuir-Hinshelwood and Eley-Rideal mechanisms, this results in the following model equation:

$$\frac{\partial \theta_i}{\partial t} = r_{adsorption} - r_{desorption} + \sum(v_{i,j} * r_{reaction,j}) \quad (4.23)$$

where r_x is different rates and $v_{i,j}$ is a stoichiometric coefficient. The stoichiometric coefficient represents the degree to which a chemical species participates in a reaction.

$$v_i = \frac{dN_i}{d\xi} \quad (4.24)$$

¹Sorption refers to the total action of both absorption (chemistry) and adsorption

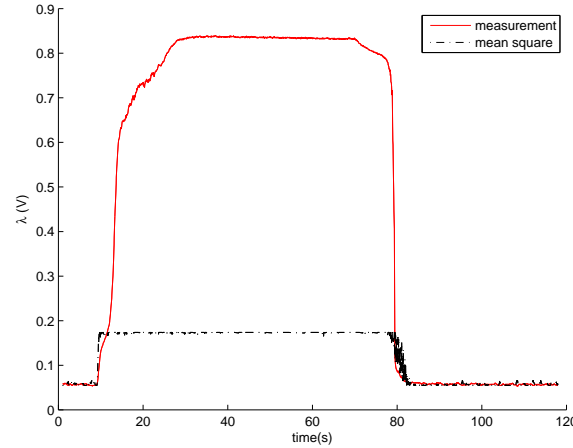


Figure 4.5: The Figure shows the second Oxygen based model versus the measure. The model is sufficient in the lean side but poor on the rich.

Where N_i is the number of molecules, and ξ is the parameterizing variable (the progress). It can be safe to assume that the adsorption rate $r_{adsorption}$ depends on the temperature, the molecular mass of the specific substance and the concentration of the same. For a substance to be absorbed there must be vacancies on the electrode, consequently making this a variable also. In addition there must be differences between electrodes in their adsorption capacity and a correction factor for this. The formula ends up as (4.25).

$$r_{adsorption} = s \sqrt{\frac{RT_{exh}}{2\pi M_i}} \frac{1}{L_{electrode}} c_i \theta_v \quad (4.25)$$

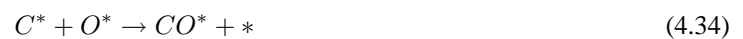
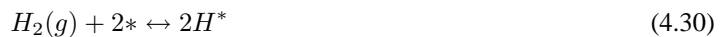
Where s is the sticking probability, which mainly is a correction factor and $L_{electrode}$ is the adsorption capacity of the electrode. The desorption rate is obtained from Arrhenius which is a surprisingly easy formula but has proven very accurate for the temperature dependency of a chemical reaction rate.

$$r_{desorption} = A_{desorption} e^{-\frac{E_{desorption}}{RT_{surface}}} \theta_i \quad (4.26)$$

$A_{desorption}$, $E_{desorption}$ is two factors that need to be determined by experiments. Although in reality there exists lists of many reactions. Note that in the above equation it's not the exhaust temperature, but the surface temperature of the surface. The reaction rate $r_{reaction}$ is modelled with the Arrhenius equation. The reaction rate is dependent on two different concentrations hence the equation becomes:

$$r_{reaction} = A_{reaction} e^{-\frac{E_{reaction}}{RT_{surface}}} \theta_i \theta_j \quad (4.27)$$

The reactions taken account for in the model used are the following:



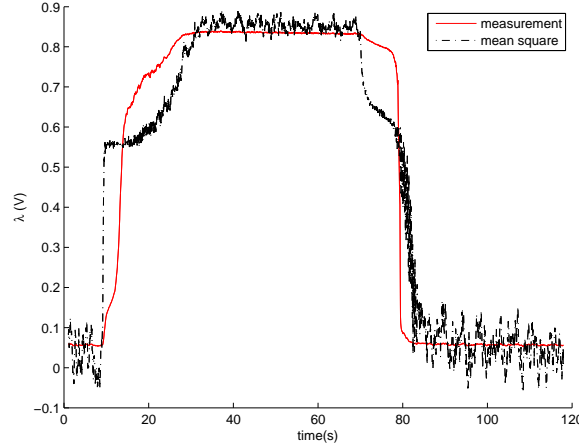


Figure 4.6: The Figure shows the extended gas model versus the measured. The resemblance is quite low, both for the rich and the lean side. The model suffers from the same shortcomings as the first oxygen based model, to high sensitivity caused by using the same least square on both the rich and lean side

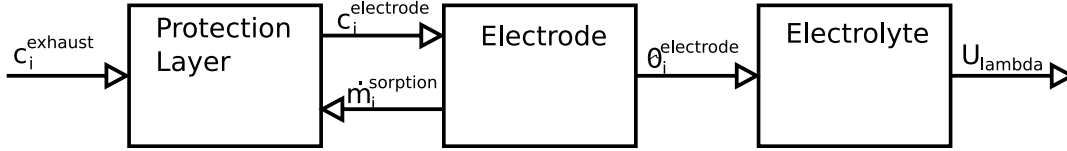


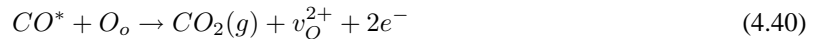
Figure 4.7: Structure of full Auckenthaler model. The model is from [3] by Auckenthaler and describes a switch type λ -sensor in detail.



Where * stands for adsorbed specie and * stands for a vacant site on the electrode. In the original model there were also reactions involving Nitrogen but as the test values lacked this gas concentration this was not accounted for in the first draft. As the model was abandoned later on this was never fixed.

Electrolyte

To model the electrolyte not only adsorbed oxygen is accounted for but also all the reducing species. It's assumed that oxygen migrates between the electrode and the electrolyte and that the reducing species react directly on the surface with oxygen.



O_o stands for a oxygen ion in the electrolyte, v_o^{2+} is a positive vacancy in the electrolyte grid and e^- stands finally for an electron. The electron current can then be expressed as:

$$\dot{n}_e = k_f \theta_V - k_a \vartheta_{V_o} \theta_O + k_{f,CO} \theta_{CO} + k_{f,H} \theta_H - k_{a,H} \theta_{OH} \vartheta_V \quad (4.42)$$

Where ϑ_{V_o} stands for the fraction of vacant sites. Assuming steady-state:

$$\begin{aligned} \dot{n}_e &= k_f \theta_V - k_a \vartheta_{V_o} \theta_O + k_{f,CO} \theta_{CO} + k_{f,H} \theta_H - k_{a,H} \theta_{OH} \vartheta_{V_o} = 0 \Rightarrow \\ \vartheta_{V_o} &= \frac{k_f \theta_V + k_{f,CO} \theta_{CO} + k_{f,H} \theta_H}{k_a \theta_O + k_{a,H} \theta_{OH}} \end{aligned}$$

The same reaction and consequently the same formula for the electron current is of course also valid for the reference side:

$$\vartheta_{V_o}^{ref} = \frac{k_f \theta_V^{ref}}{k_a \theta_O^{ref}} \quad (4.43)$$

Although naturally only oxygen is accounted for on this side. These two equations can now be inserted in the nernst equation (4.19):

$$E = \frac{kT}{e} * \ln \frac{\theta_O^{ref} (\theta_V + \frac{k_{f,CO}}{k_f} \theta_{CO} + \frac{k_{f,H}}{k_f} \theta_H)}{\theta_V^{ref} (\theta_O + \frac{k_{a,H}}{k_a} \theta_{OH})} \quad (4.44)$$

In Figure 4.8 the result from the model is seen. The resemblance is rather poor, specially the signal seems very noisy or instable. Also worth noticing is that the model suffers from bad behavior during transients. The step from lean to rich is much too fast.

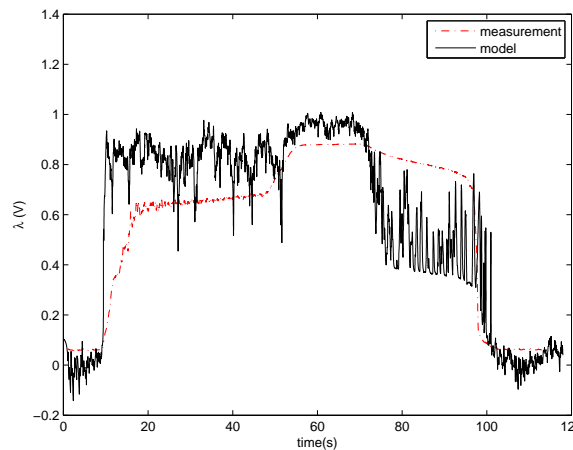


Figure 4.8: The results from the Full Auckenthaler model. Although the model seems promising it leads to poor performance in this test. Worth noticing is the problem with transients, the step from lean to rich is much too fast.

4.2.4 Simplified Auckenthaler

In [3] Auckenthaler also describes a simplified variant of the above stated model. This model is mainly derived for using in a control system. This model is based on the above *Full Auckenthaler* model but has been refined and optimized regarding complexity and speed. The model is implemented in [9] as a runnable Simulink model. The result can be seen in Figure 4.9 and shows good resemblance. The only problem is the step from lean to rich which is too fast.

4.2.5 Simplified Auckenthaler with diffusion

This model is a refinement of the above. To relieve the problem with the lean to rich step, a diffusion model is introduced. The diffusion is modeled using a simple first order system. To get a higher accuracy the system can be modified with a time constant dependent on temperature and pressure. Furthermore to get different substances to diffuse at different speed the time constant can be dependent on mole mass. The simplified Auckenthaler model assumes that the HC and NO_x concentrations are present. This is not the case for all test values available and the model is therefore modified. O_2, CO and H_2 are the most important gases for this thesis so this is acceptable. HC and NO_x is approximated with a linear dependency of CO and O_2 . Figure 4.10 shows the resulting model and the measured values. Both of the models shows great resemblance, although the model with a time constant dependent on the mole mass is slightly better. This model is also tuned slightly resulting in a better midpoint.

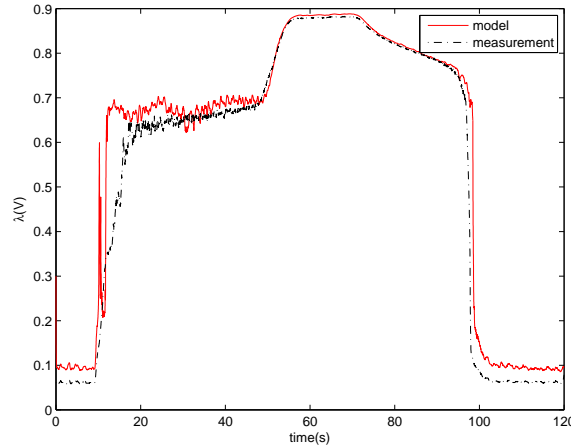


Figure 4.9: The Figure shows the results from the Simplified Auckenthaler model. Notice the too fast step from lean to rich.

Conclusion

The linear regression models are all very simple and easy to deal with but they all have an overall low resemblance with the real world. This is because of tremendous simplifications made. The *oxygen based models* (and specially *oxygen based model 2*) has very good resemblance as long as the mixture is lean. The conclusion drawn is that the sensor is mainly driven by oxygen on the lean side and likewise as the resemblance is quite low on the rich side that oxygen hardly affects the output at all on the rich side. Not only do the *oxygen based models* have low resemblance but also the *extended gas model* has the same appearance. The conclusion drawn from this is that although the most important gases are present in the linear approximation, it's not enough. One suggestion for a model is to only use O_2 on the lean side where it is proven to be good and then using the reducing species H_2 and CO on the rich side. This is of course cheating, because the λ -value must then already be known. The result can be seen in Figure 4.11. The Figure shows much greater resemblance but is still far from perfect. This means that a simple linear approximation isn't good enough and another approach is justified. Although the simple linear regression models failed there is no use to expand these with higher grade polynomials. The advantage with these are their simplicity which then would be lost. Instead it's better to try to base the model on physics. With this approach the model also gets more portable. One conclusion drawn from the linear regression models is that on the lean side the sensor is mainly Oxygen driven and on the rich side the sensor is mostly sensitive for Hydrogen and Carbon Oxide. Also no single gas is enough to describe the sensor accurately. This retires the term oxygen sensor.

The *full Auckenthaler* model is very promising in [3] but the results weren't to satisfaction in this thesis. This is because of the complexity of the model, which also is its biggest flaw. In a quality point of view this is probably the best model tested, but with 50 different variables in the model the job to tune them gets to big for this thesis. In addition the diffusion step was never implemented because of limited time, this probably affected the model very badly.

The real strength with the *simplified Auckenthaler* model is its simplicity, there are no complex math operations but still it has a good congruence. The resemblance at fast rich to lean step is low, this is really bad for the wide band model. One of the reasons for the unstable output at some parts are the discontinuities that the model introduces. This is always the risk when using two different models for different intervals of the model. In this case one for the rich side and one for the lean side. The *simplified Auckenthaler with diffusion* model introduces a diffusion step to calm the discontinuities in the *simplified Auckenthaler* model. The too steep rich to low switch seen both in *simplified Auckenthaler* and in the *full Auckenthaler* model (where no diffusion step was implemented) was fixed with the diffusion. The *simplified Auckenthaler with diffusion* model has more than enough accuracy for the wide band model and is therefore used.

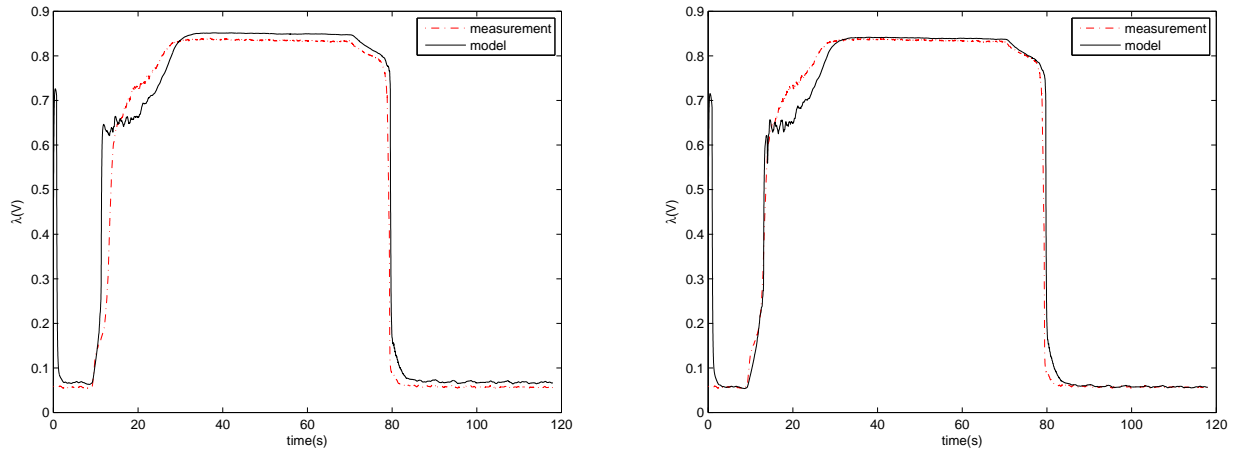


Figure 4.10: The left Figure is the simplified Auckenthaler with a first order system with a non-variable time constant. The right Figure shows the system with a time constant dependent on mole mass. In this Figure the middle point has also been adjusted resulting in a better midpoint.

4.3 Diffusion

To model the diffusion for the wide band sensor the same algorithm as the switch-type diffusion is chosen. This involves a simple first order linear system with a time constant dependent on the square root of the mole mass. The effect of the system can be seen in Figure 4.12 where the absolute difference between the input and the output is displayed. As expected the model function like a low-pass filter.

$$\frac{\partial c_i}{\partial t} = (c_{i,in} - c_{i,out}) * \frac{1}{\sqrt{M_i}} * K_{diff} \quad (4.45)$$

4.3.1 Results

This algorithm works very well in the switch type sensor, however in the wide band model it isn't optimal as the diffusion is much more complex [3], especially the dependency on the mole mass and the temperature (which in this model is assumed to be constant). Because of limited time this model is chosen anyway. A much better alternative would be to implement the diffusion described in [3].

4.4 Oxygen Pump

In a real wide band sensor the oxygen pump is actually just a nernst cell with an external applied current. The most important formula for this block is (4.46) [5] [11], with this mole quantity is easily calculated from the pump current.

$$n(O_2) = \frac{i * t}{4F} \quad (4.46)$$

Where i is the pump current and F is Faraday's constant. The reason for pumping out oxygen is to achieve equilibrium in the cavity. For a lean mixture there's nothing more to it, the sensor controller will pump out just enough oxygen. For a rich mixture it's a little more complicated, more oxygen is needed in the cavity but the oxygen level in the exhaust is extremely low. Fortunately when applying a negative current to the pump, water and carbon dioxide in the exhaust gas is reduced to hydrogen and carbon oxide.



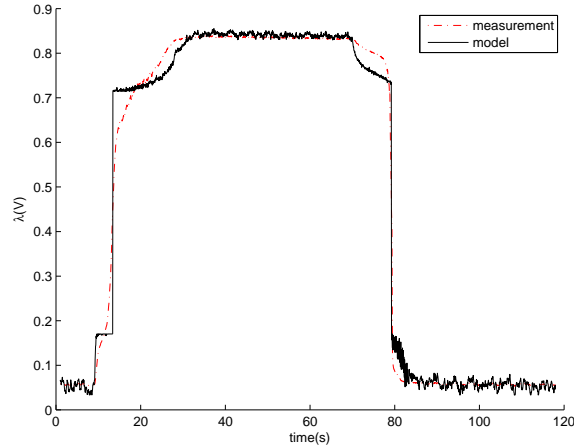


Figure 4.11: The Figure shows a modified Linear regression model. The λ -value is assumed to already be known and used to decide what equation to use for different parts of the graph. When the output is lean the model only uses O_2 as input and corresponding when the output is rich the model uses CO and H_2 .

In the cavity the opposite reactions occur and equilibrium is achieved. The equilibrium is also driven by the water-gas shift reaction. In Figure 4.13 the difference between two test runs is shown. Especially notice the λ -value and it's correlation with the CO and H_2 concentrations. It's easily noticed that the CO and H_2 effect on λ is not equal [10]. Therefore two constants must be introduced, see equation (4.49). Note the minus sign, oxygen is pumped into the cavity.

$$I_{pump}|_{\lambda < 1} = -k_{CO}[CO] - k_{H_2}[H_2] \quad (4.49)$$

Concentration is not allowed to be negative, if the controller tries to pump out too much oxygen the level saturates at zero. It's assumed that equation (4.47)-(4.48) is valid so instead the CO and H_2 concentration goes up.

4.4.1 Results

The change in partial pressure for different pump current can be seen in Figure 4.14. The different slopes of the gases reflect their respective sensitivity.

4.5 Regulator

As a regulator a simple PI-regulator is used, also a first order linear system is used to simulate the speed of the controller. The system is considered to be too slow to need a derivative part, in addition the system gets a smaller overshoot.

4.5.1 Results

The regulator could have been implemented in a much more sophisticated way, perhaps with a kalman-filter. The regulator is using a PI-regulator for two reasons: First this thesis concentrates on static errors, not dynamic, and second it's impossible to know how the real controller regulates therefore a simple algorithm is chosen.

4.6 Lambda generation

From the pump current the lambda value must be calculated. A normal output from a wide band λ -sensor is seen in Figure 3.6, this must be translated to λ .

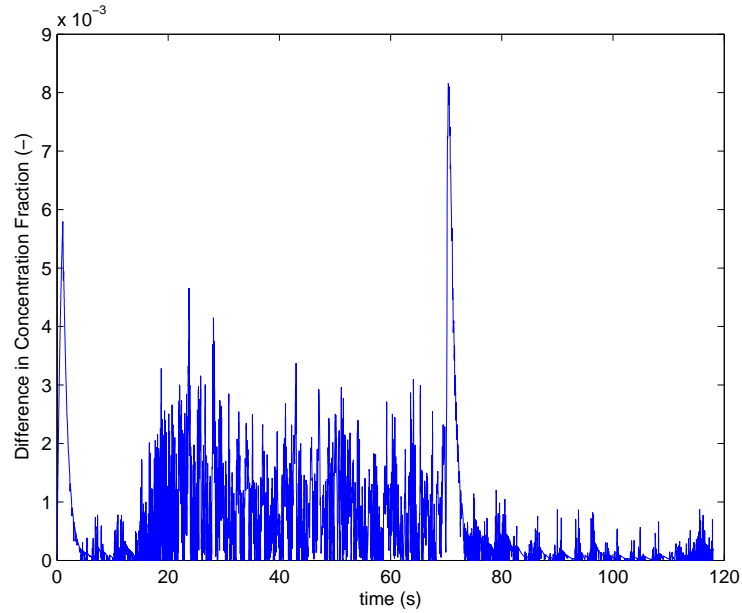


Figure 4.12: The diffusion's effect on CO concentration. As the diffusion is modeled by a first order system the result is a low pass filter.

4.6.1 Brettschneider

To be real accurate the Brettschneider equation (4.50) can be utilized [1]. This function relates concentrations of gases with λ .

$$\lambda = \frac{[CO_2] + [\frac{CO}{2}] + [O_2] + [\frac{NO}{2}] + ((\frac{H_{CV}}{4} * \frac{3.5}{3.5 + \frac{[CO]}{[CO_2]}}) - \frac{O_{CV}}{2}) * ([CO_2] + [CO])}{(1 + \frac{H_{CV}}{4} - \frac{O_{CV}}{2}) * ([CO_2] + [CO]) + (C_{factor} * [HC])} \quad (4.50)$$

Where $[XX]$ is the gas concentration in volume percent, H_{CV} is the atomic ratio of hydrogen to carbon in fuel used, O_{CV} is the atomic ratio of oxygen to carbon in fuel used and C_{factor} is the number of carbon atoms in each of the HC molecules. Equation (4.50) can not be used directly as most of the gases are unknown, however with the λ -value from the sensor together with injected fuel and air all the concentrations can be guessed with high accuracy.

4.6.2 Lookup table

The easiest variant is to use a lookup table with interpolation in between, creating a piecewise linear function. Figure 4.15 shows an example when fitting the actual curve produced of the model with a piecewise linear function. The points used when fitting is easily spotted. Figure 4.16 shows the error introduced when using a piecewise linear function. As expected the error is zero at the points used when fitting. The maximum error seen in the Figure is around 0.0035. The model will be used when evaluating errors in the range from 0.005 – 0.015, this makes the 0.0035 to much. However as the model will be used to compare two test runs the resulting error will be less. If

$$\lambda = i * f(i) + e(i) \quad (4.51)$$

where i is the pump current, $f(x)$ is the function relating i to λ and $e(x)$ is the error introduced with a lookup table. Then the difference between two test runs is consequently $\lambda_1 - \lambda_2 = i_1 * f(i_1) - i_2 * f(i_2) - e(i_1, i_2)$.

$$|e| = |e(i_1, i_2)| = |e(i_1) - e(i_2)| \leq |e(i_i) - e(i_2)|_{max} = |e(i_i) - e(i_1 + x)|_{max} \approx 0.002 \quad (4.52)$$

Where x is the error range 0.005-0.015. The maximum error introduced with the lookup table is therefore 0.002. In reality most cases will produce a much smaller error. Also as the error range is under 0.015 the resulting

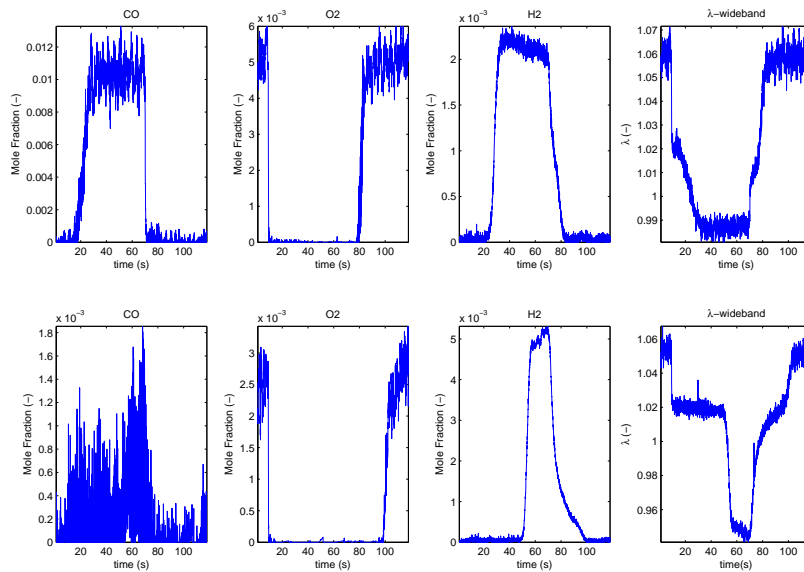


Figure 4.13: The Figure shows the gas concentrations for test run 1 and run 3. Especially notice the λ -value and it's correlation with the CO and H_2 concentrations. As the sensitivity for CO and H_2 appear to be different the pump circuit must be modified to reflect this.

distortion will in most cases be increased or decreased swing for the error, i.e the shape of the error will not be distorted.

4.6.3 Conclusion

The Bretschneider equation gives certainly the best result but is very complex. The best approach is therefore the table approach. It has problems with introduced errors but in this case it's acceptable. Besides the behavior of the real controller is unknown so an easy approach can as well be used.

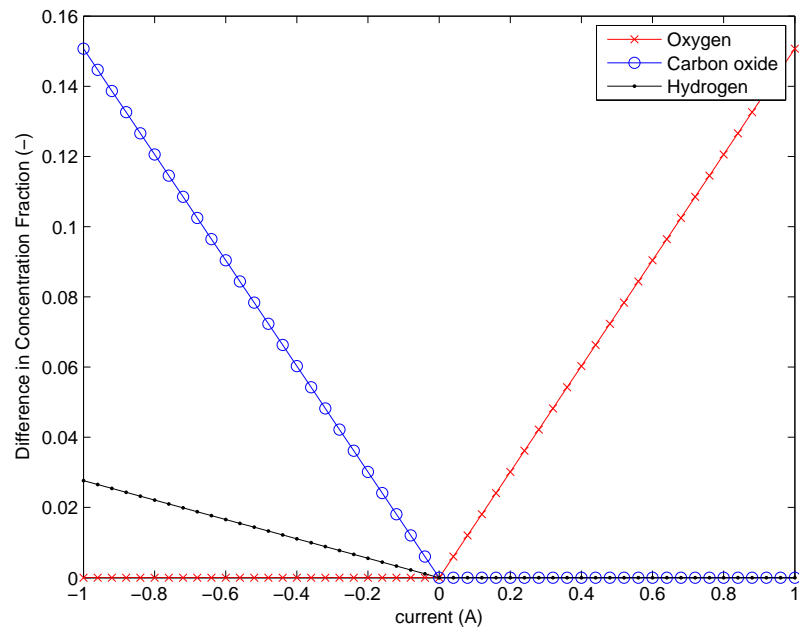


Figure 4.14: The Figure shows how the partial pressure inside the cavity changes for a ramp in pump current. Note that a negative current has different effect on CO :s and H_2 :s partial pressure.

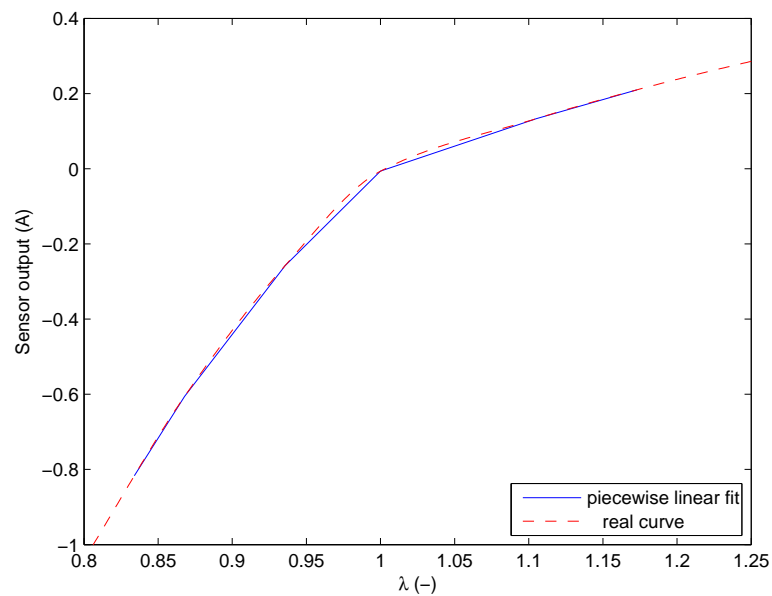


Figure 4.15: The Figure shows an example when fitting the actual curve produced of the model with a piecewise linear function. The points used when fitting is easily spotted.

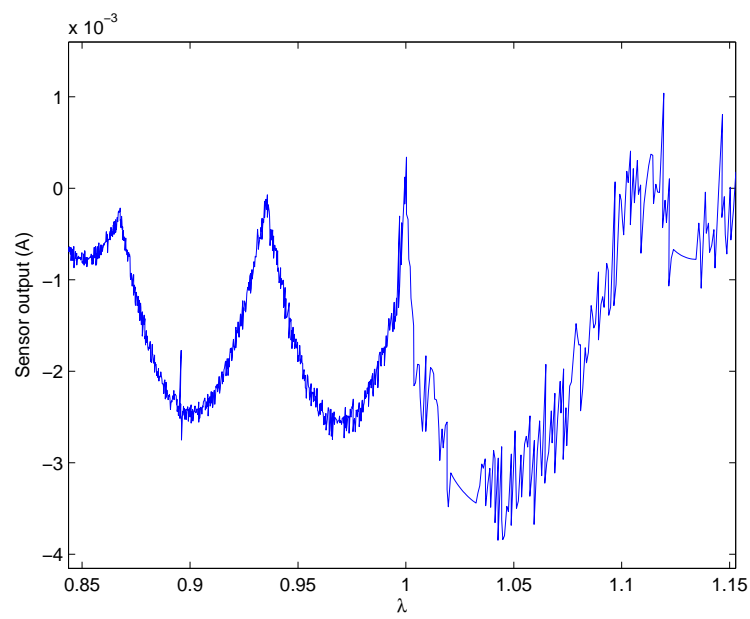


Figure 4.16: The Figure shows the error introduced when using a piecewise linear function. The points used when fitting is easily spotted as the error is zero at their locations.

Chapter 5

Validation of wide band model

This chapter describes the results from the model developed in the preceding chapter.

5.1 Test setup

Unfortunately there is no simple way to run exactly the same test on the model as in the real engine setup, the lack of a gas analyzer prevents this. Without an apparatus of this kind it's impossible to know the gas composition during the test runs, which is needed by the model. Therefore the tests concentrate on the general principle of the results, rather than comparing exact values. In some cases the developed exhaust model has been used to estimate the gas composition. Another fact that complicates the tests is that no data includes exhaust pressure or temperature.

5.2 Testing of the model

First of all the models accuracy itself needs to be tested. The model is tested with all of the data available, namely the developed exhaust model and the two real test runs available [15].

5.2.1 Calibration

As no data include pressure or temperature, these must first be set with reasonable values. Where it has been needed in this chapter the pressure is assumed to be $100kPa$ and the temperature $700K$. After this the sensitivity for H_2 and CO must be decided or at least the size of their fraction as the actual size is compensated for by the PI-controller. Then the pump current to lambda lookup function must be calibrated. This is most easily done by simulating the system once and then comparing the pump current from the model to the measure lambda output. It should be noted that the calibrations done on the model is in no way optimal. The aim wasn't a model with exactly correct values but one with correct behavior, therefore little time has been spent on this.

5.2.2 Exhaust gas Model

The first test compares the output of the model with outputs from the exhaust model. Figure 5.1 shows the result for different λ -values. As the wide band model is calibrated against the output of the exhaust model it's always possible to get a good result if enough points is used when fitting the lookup table. However during this test only 5 values is used.

5.2.3 Real Test Data

This test uses the the test data from [15] (see Appendix A). The data contains two usable test runs, these and their corresponding output from the wide band model can be seen in Figure 5.2. The model is calibrated for the left Figure using only 4 values.

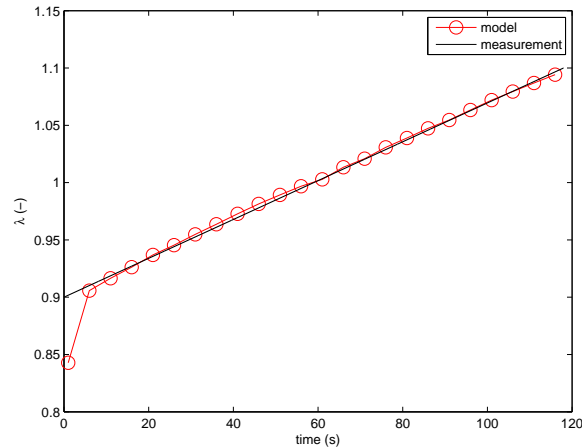


Figure 5.1: The Figure displays the output from the wide band model against the output from the exhaust model. 5 values is used in the lookup table.

5.2.4 Results

The model shows great resemblance with the input, therefore it's concluded that the model works for a static temperature and pressure input. The model does however takes some time to settle first, this could be improved. In addition the real test values are from *after* the catalytic converter, this is harder to model because before the catalytic converter the concentration of CO correlates to H_2 for a specific lambda. After the catalytic converter there is no such reliable relation making it harder to get a unified model. The model could be suspected to have problems with fast switches between lean and rich (see right Figure in 5.2). The diffusion step might introduce this error but it could just as easily be calibration related.

5.3 Pressure

In [5] it's suggested that the uego sensor output is dependent on pressure. Unfortunately no test data include pressure input, instead a normal pressure of $100kPa$ is assumed for all test values. In Figure 5.3 the difference in output for different pressures can be seen. The top two Figures show the output from the model when changing the pressure. The left one shows the output when feeding the model with higher pressure and the right shows lower pressure. 10 and 20 percent over- respective under- pressure is used. The lower Figure shows the difference in lambda from an output with normal pressure against one with higher/lower pressure. The Figure is resorted to be over λ instead of time. A test run on a real engine was also made, in this test the exhaust pressure is held high by choking the exhaust pipe. The injection time as well as air flow is held constant over time. When enough samples are recorded the choking is released and the new equilibrium is given time to settle before finishing the test. The resulting λ -value and exhaust pressure can be seen in Figure 5.4.

5.3.1 Results

The implication from the model is clear: The higher pressure the sensor is exposed to, the more swing is outputted. At roughly $\lambda = 1$ the output is unaffected. However in reality the relation seems not that easy, the λ -value seems to get richer when lowering the pressure, irrespective of a lean or a rich mixture. As both the steps (Figure 5.4) looks similar the nearest conclusion is that the difference seen is actually something else. If this is true the conclusion drawn is that the diffusion into the sensor is not pressure driven. This means that the pump model need to change to reflect this.

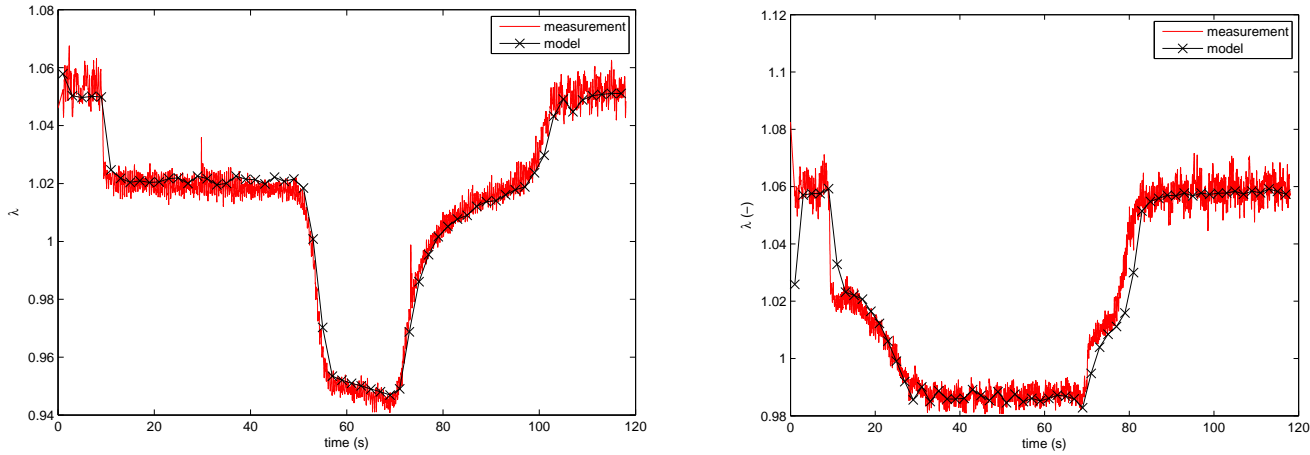


Figure 5.2: The Figure displays the output from the wide band model against the measure. The model is calibrated for the left Figure.

5.4 Temperature

No temperature effect was considered due to the too simple diffusion model in the wide band model. Normally the diffusion is highly dependent on temperature but this is not considered at all in this model, therefore it seems meaningless to do any calculations (although the switch model is actually dependent on temperature). Neither sensor temperature or exhaust gas temperature has been considered to a fully extent.

5.5 Improvement of UEGO model

As always improvements can be made. This section lists suggested improvements for the future, they are divided into three subsections.

5.5.1 Diffusion

The model's weakest link is the diffusion step. For now the diffusion only works as a low pass filter but with different cut-off frequencies for different substances. In reality the diffusion is dependent on both temperature and pressure. A good approach would be [3].

5.5.2 More data

The model should also be tested with a sufficient amount of data, this has been a problem during the whole thesis. Without more data the risk is that the model only works for a specific test. This however is not likely with this model as it passes test from *after* the catalytic converter with different aging. Thereby having different gas compositions.

5.5.3 More gases

The model design only lets oxygen, hydrogen and carbon monoxide influence the output, it has been shown [3] that at least hydrocarbons and nitrogen oxides also has effects on the sensor.

5.5.4 Better pressure tests

The model needs to be further tested against the real world for pressure sensitivity. If, the results from Section 5.3 are true, the model need to change to reflect this.

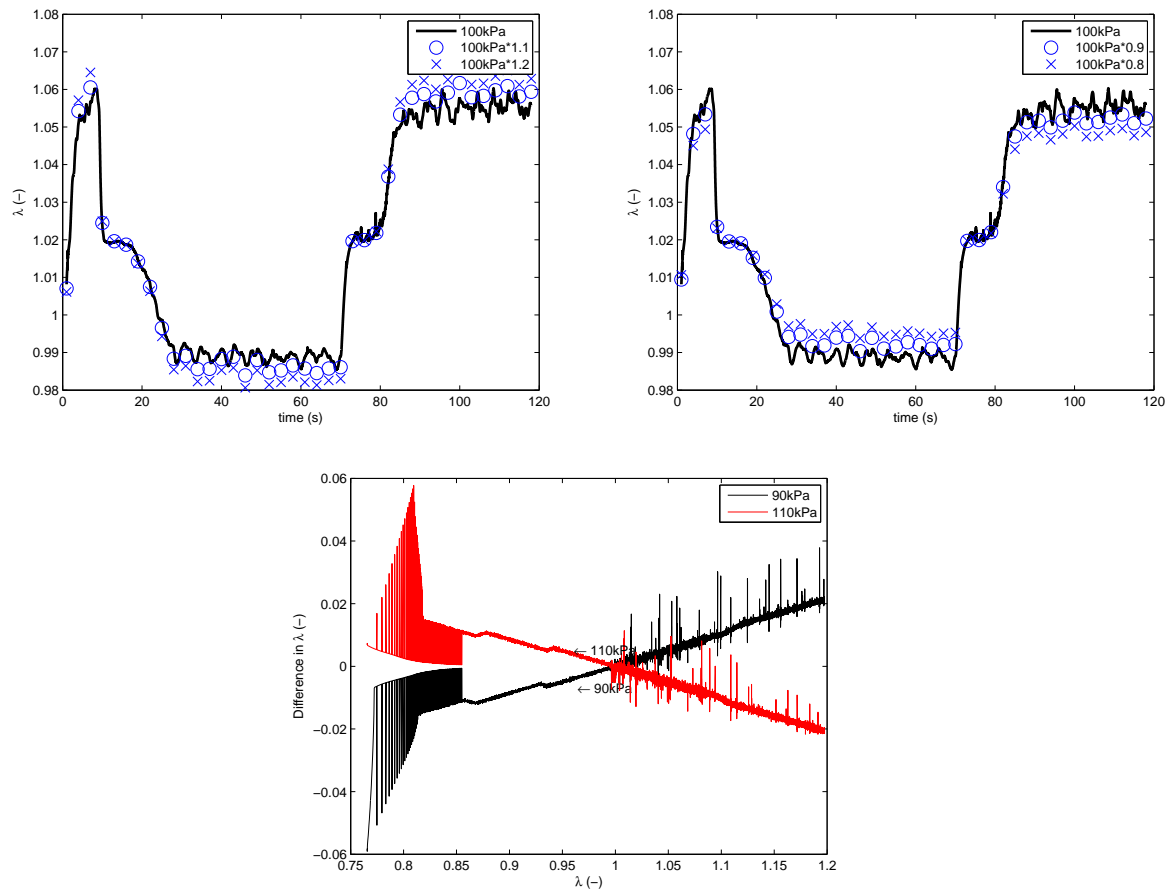


Figure 5.3: The top two Figures shows the output from the model when changing the pressure. The lower Figure shows the difference in lambda from an output with normal pressure against one with higher/lower pressure.

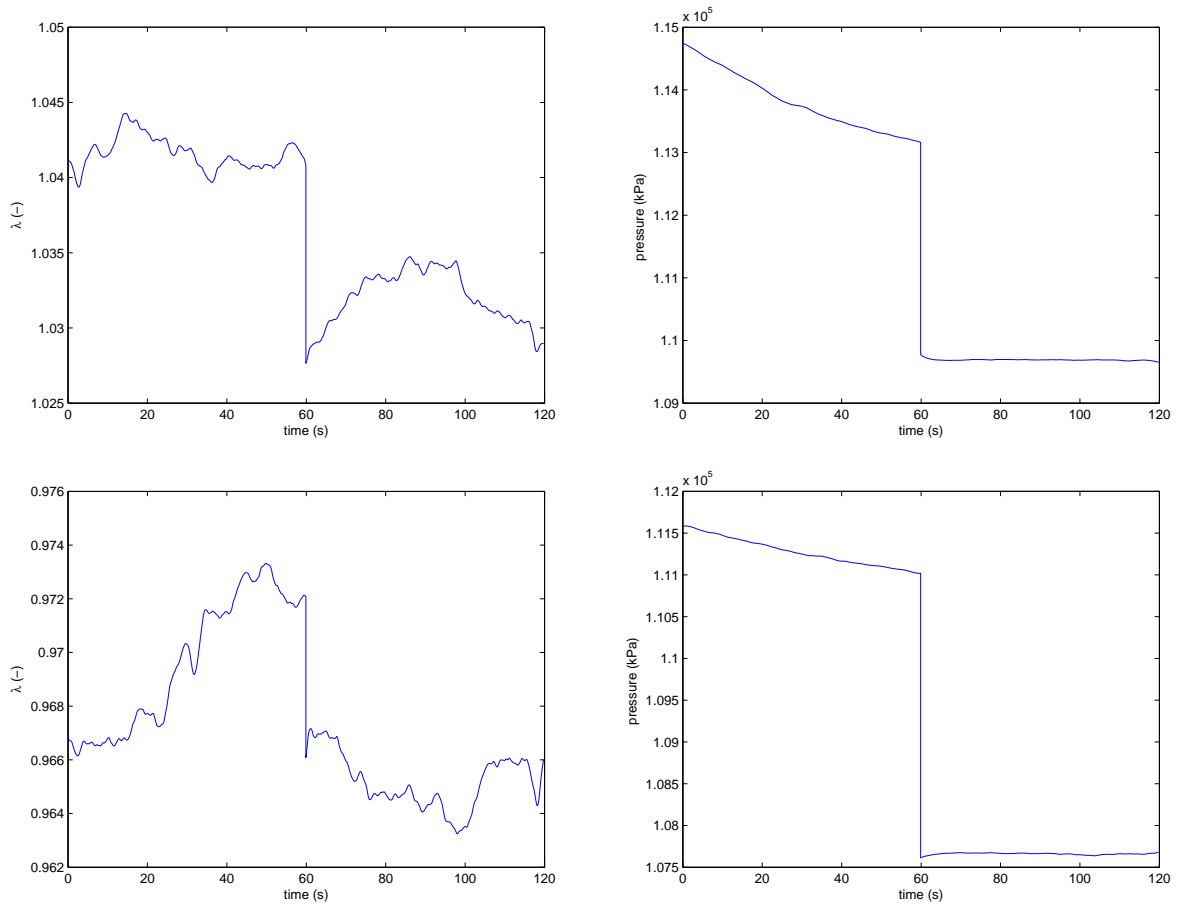


Figure 5.4: The Figure shows the results from a test run looking for changes in λ when pressure was changed. The injection time and air flow is held constant over time where as the pressure is changed.

Chapter 6

Observer

This chapter deals with the development and the implementation of the observer.

6.1 Problem

The function of a wide band λ -sensor is much more complicated than a discrete type, therefore it's much harder to get correct readings. The goal is to develop an observer to minimize the error when using this kind of sensor. The model of the wide band λ -sensor is used to evaluate different problems in preparation for the observer. To evaluate the problems and their ability to explain differences between real life lambda and a sensor output, two sensors with differing output have been used as an example. Several potential problem sources are tested and investigated, these include calibration error, pressure error, air leak error, gas sensitivity and fuel errors. The upper left picture in Figure 6.1 shows the output from the two different sensors during a test, the upper right shows the difference. It's assumed that the error is time invariant so therefore the error is modified to be over λ instead. This can be seen in the lower left picture in the Figure. The lower right picture shows the same but all extreme values removed and a straight line fitted.

6.1.1 Exhaust gas model tests

To test what kind of difference in output that arises from different errors, the gas model developed in Section 4.1.1 is used. First the output from one of the lambda sensors is fed through the exhaust model and the resulting gas output is used for testing. This way the test from 6.1 gets available with the gas composition approximated. This test are called *exhaust gas model test* through out of his chapter.

6.1.2 R_{cal} error

One possible error for a wide band sensor is the calibration resistor R_{cal} . The resistor is used in car industry for calibration purposes, however for high quality measures this calibration can be insufficient. In addition the resistor is included in the wiring harness and is exposed to both high temperatures and moisture, this will age the resistor and ruin the calibration. The extra wires for the resistor might also introduce common-mode noise to the channel, although the controller will likely use a differential amplifier to measure the current this will still introduce a small error. This kind of error can also be related to a bad or faulty electrical connection. Figure 6.2 shows how the resistor is connected. The controller expects a value of $R_{in} \parallel R_{cal}$ as input resistance for the differential amplifier, if instead the R_{cal} has an error and has the value $R_{cal} * R_e$ the total error becomes:

$$error = (R_{cal} * R_e) \parallel R_{in} * \frac{1}{R_{cal} \parallel R_{in}} \quad (6.1)$$

$$= \frac{R_{cal} + R_{in}}{R_{cal} * R_e + R_{in}} \quad (6.2)$$

For this test it's safe to assume that the $R_{in} \approx R_{cal}$ which ends up in:

$$\frac{R_{cal} + R_{in}}{R_{cal} * R_e + R_{in}} = \frac{2}{R_e + 1} \quad (6.3)$$

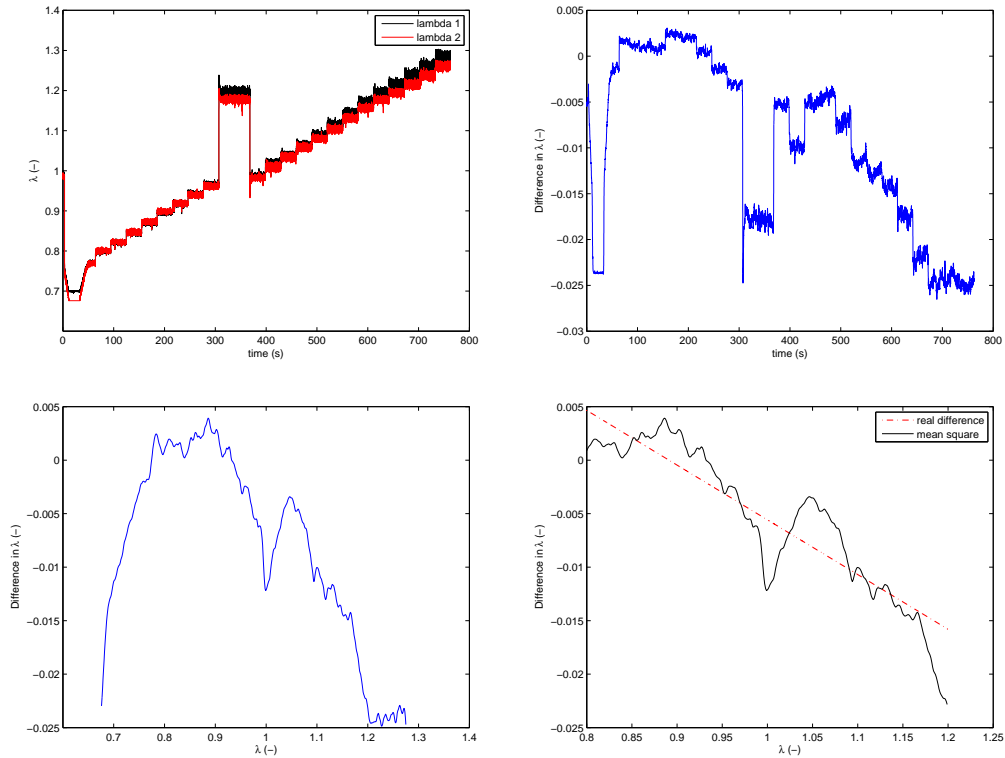


Figure 6.1: The Figures display the difference between two λ -sensors during a test. The upper left Figure shows the output from the sensors where as the upper right shows the difference. The lower left and right Figures shows the difference over λ instead. In the lower right Figure all extreme values are removed and a straight line fitted.

This error is introduced just before the lambda lookup function causing it to have an offset error. A ramp with different λ -values is run through the exhaust gas model and fed to the wide band model. This is done four times with different resistances ($0.8 \cdot R_{original}$, $0.9 \cdot R_{original}$, $1.1 \cdot R_{original}$ and $1.2 \cdot R_{original}$), the difference against a test run with $R_{original}$ is shown in the left Figure 6.3. The right Figure shows the difference between an exhaust model test with $R_{original}$ as resistance and $0.9 \cdot R_{original}$ respective $R_{original}$ and $1.1 \cdot R_{original}$.

6.1.3 Pressure error

Although the results from the last chapter states that the models pressure dependency isn't correct, to be on the safe side the second suggested error is a pressure error. Since the two sensors are placed next to each other the pressure should be the same for the both, although some spikes might occur. However in the test, Section 6.1, the engine runs at the same injection time too long for the problem to be spikes. The idea is therefore that the two sensors have different sensitivity for pressure. For this idea to work there must be a pressure difference during the original test, which can be seen in Figure 6.4. The left Figure shows the pressure difference over time, note that the difference is quite big. The right Figure shows the pressure difference resorted to be over λ instead. The conclusion drawn is that the pressure difference has something to do with mixture strength, for example observe the sudden reaction in the left picture at $t \approx 310$, this sudden spike can be derived from the sudden spike in injection time observed in Figure 6.1 (the upper left Figure). However the major part of the difference is something completely different, the reason is left to find out. Two exhaust gas model tests are used: The first with an exhaust pressure of 100k Pa simulating the least sensitive and the second with the real pressure difference normalized to 100k Pa. The difference between the two can be seen in Figure 6.5, also seen is the same difference but over λ instead. This assumes that the error is time invariant which is not obvious when looking at Figure 6.4.

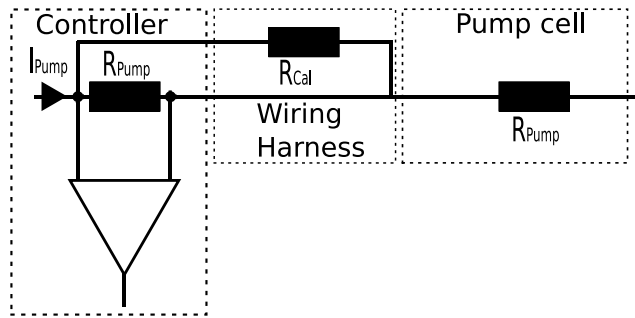


Figure 6.2: Most wide band sensors comes with a calibration resistor connected like in the Figure. Over time the resistor will age and ruin the calibration.

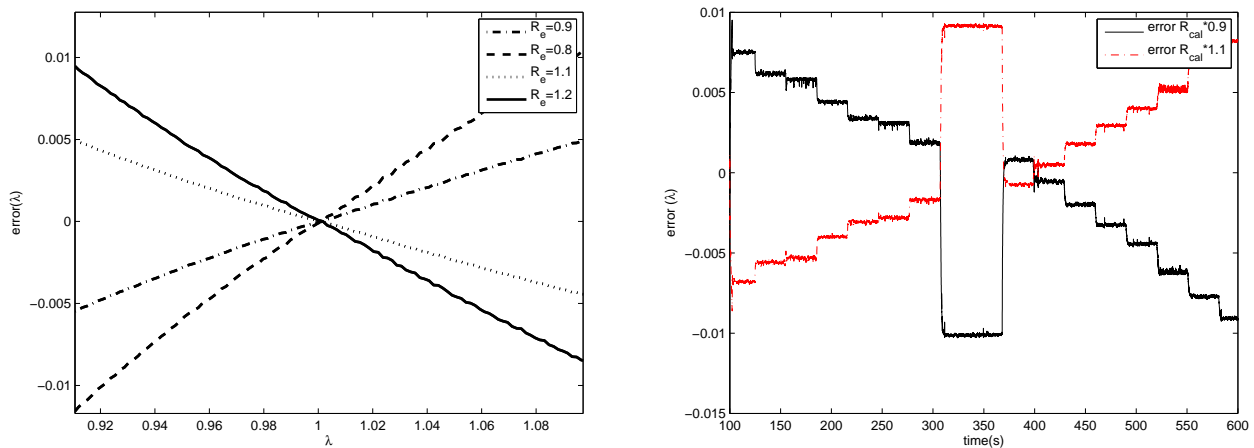


Figure 6.3: The difference in output from the wide band model with different values for the calibration resistance against the original resistance is shown in the left Figure. The right shows the same but during a test when the exhaust model is used.

6.1.4 Temperature error

The temperature effects has been left out as the non-existing temperature effects in the diffusion step see Section 4.3 and the degraded temperature effects on pump current.

6.1.5 Air leaks error

The fourth error tested are air leaks (or faulty air injection) [1]. This is modeled by a static oxygen fraction increase of 0.005. A exhaust gas model test is performed and the results is shown in Figure 6.6.

6.1.6 Different gas sensitivity error

The two sensors could of course experience different sensitivity for every gas but only CO, H_2 and O_2 have been explored here. This is because they are the only three gases accounted for in the model.

CO and H_2 sensitivity

These two gases are reducing and are almost zero when $\lambda > 1$, therefore they are not probable causes for any differences between the sensors for this inequality. The error is assumed to be on the form $error = k_1 * [XX] + k_2$ so a least square is fitted to the output from a synthetic test. Both the real difference and the least square is shown in Figure 6.7. The error could also be on the form $error = k_1 * [CO] + k_2 * [H_2] + k_3$ and hence be dependent

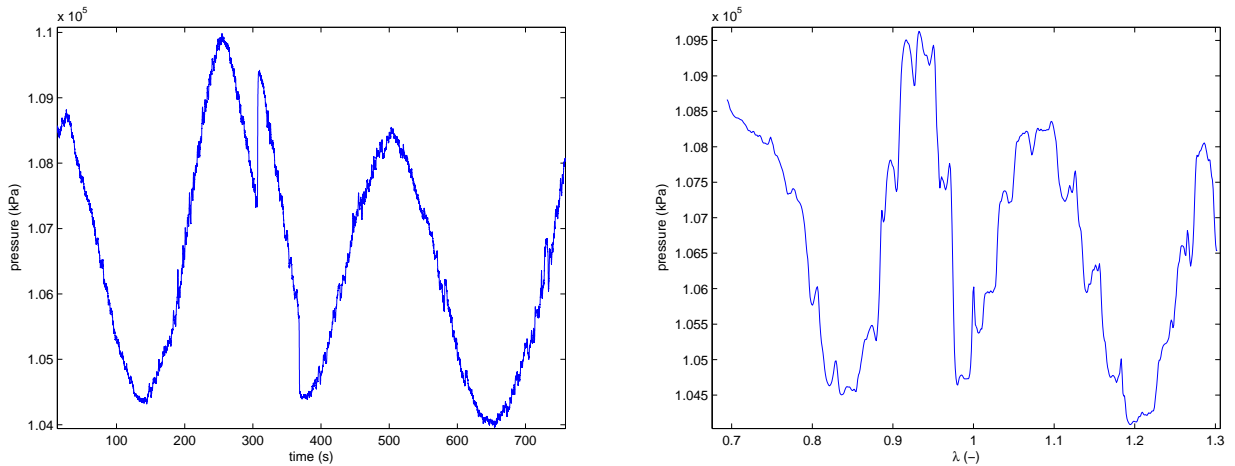


Figure 6.4: During the test from Section 6.1 the wide band sensor experienced variations in the pressure. The left Figure shows this variation over time and the right shows the same over λ .

on both carbon oxide and hydrogen. Figure 6.8 displays the result from a mean square assuming this form.

O_2 sensitivity

O_2 is almost zero when $\lambda < 1$, therefore it's not likely to cause any difference between the sensors for this inequality. The error is assumed to be on the form $error = k_1 * [O_2] + k_2$

The test is performed as in the previous section. Two tests are performed, one where the entire range $\lambda > 1$ is used as input to the least square and one where only $\lambda > 1.05$ is used. The later is tested due to the inaccurate behavior of the exhaust gas model when λ approaches 1 and at misfire. Both are seen in Figure 6.9.

6.1.7 Fuel difference error

If the fuel type change, the output from the lambda sensor will also change (different fuel combustions give different equilibrium equations). To test if the problem might be fuel related a test with 20% ethanol is added to the normal fuel, assumed to be octane C_8H_{18} . A test using the exhaust model is performed for each fuel and the difference between them is shown in Figure 6.10.

6.1.8 Conclusion

R_{cal} error can be ruled out as the major source, this error doesn't has any offset at $\lambda = 1$. Of course this doesn't mean that it couldn't account for secondary effects. The Pressure error can also be ruled out with the same argument as the R_{cal} error, no offset at $\lambda = 1$. In addition the error looks definitively wrong over λ . The Air leak error does have a reasonable offset error at $\lambda = 1$ but the error on the lean side is wrong. The real error has a slope that this error misses. This concludes that this cannot be the only error anyway. The Different gas sensitivity error shows some interesting results. On the lean side $\lambda > 1.05$ the error is roughly explained by a function like $k_1 * [O_2]$. The reason for the bad congruence at $1 < \lambda < 1.05$ could be explained by the exhaust model. It should be noted that the exhaust model which is used here is not at all suited for this kind of use. The model only approximate the real gas concentrations with a rough linear method. Especially for extreme values and around $\lambda \approx 1$ the model is ill-suited. At $\lambda = 1$ the model changes gas concentration very abruptly where as a real engine is more complex as both the reducing species CO and H_2 is present as well as O_2 . The rich side error on the other looks like it's explained with a function of $k_1 * [CO] + k_2 * [H_2] + k_3$. The reason for why the fuel difference error cannot be the only error is the amplitude, this error only shows a tenth of the amplitude from the real error.

All in all the best suggestion with the available tools and tested error is that the error is a gas sensitivity error. If the sensors have different sensitivity for different gases, the explanation for this could be one or more of several

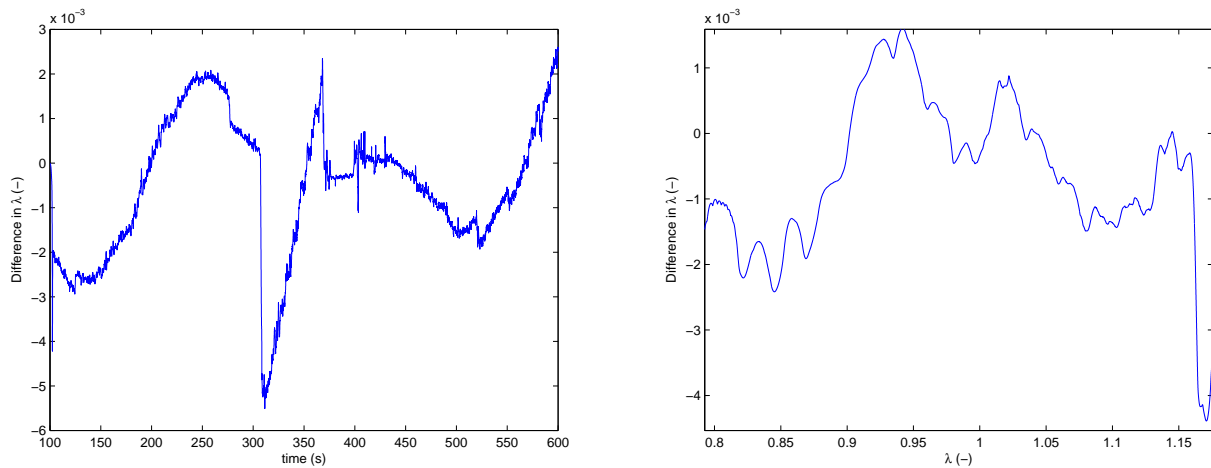


Figure 6.5: The Figure shows the difference between two outputs from the wide band model, which differs in their sensitivity for pressure. The left is in the time domain and the right is in the λ -domain.

aspects: The nernst cell could be different, the pump cell could be differently good to pump out different gases between the two sensors or even the diffusion step could be responsible. This is not investigated any further.

6.2 Solution

It's very hard to examine the error deeper without a gas analyzer present. This leads the solution onto an other path. As the engine's running at $\lambda \approx 1$ most of the time this is the most important part to get right. The error increases as the λ diverge longer and longer from $\lambda = 1$ but if an offset is added to make $\lambda = 1$ right the error would be almost zero around 1.

When using a static offset it need to be calibrated once in a while to to rely on it. The best thing would be to have this automated, for this a second sensor is needed. A switch type sensor is perfect for this job, it is very reliable to measure lean or rich and can therefore be used to find out exactly where the switch is.

6.3 Matlab/Simulink Model

Before implementing the observer in the ECU it's meticulously tested in a model written in Matlab and Simulink.

6.3.1 Observer Model

The observer should only take information from the wide band sensor when the switch type sensor has its switch. This can be done with a sensitivity vector, however to prepare to the next step (next section) this is done by an "enable port" in Simulink. This enables the observer only when the input is greater than zero. This port has its input connected to a switch detection circuit. When the value of the switch type sensor is on the other side of the switch than the last one, this circuit gives a pulse out. In addition an one-shot block is used to avoid the pulse to last over several iterations. The overview is seen in Figure 6.11.

In Figure 6.12 the output can be seen from the observer during a test. The switch type input is during the entire test fed with a continuously switching signal. This makes the observer's output approach $\lambda = 1$ irrespectively of what the value really is.

6.3.2 Running Average Model

An observer is not suitable for ECU programming, therefore a running average model was developed. The scheme for the model is shown in Table below.

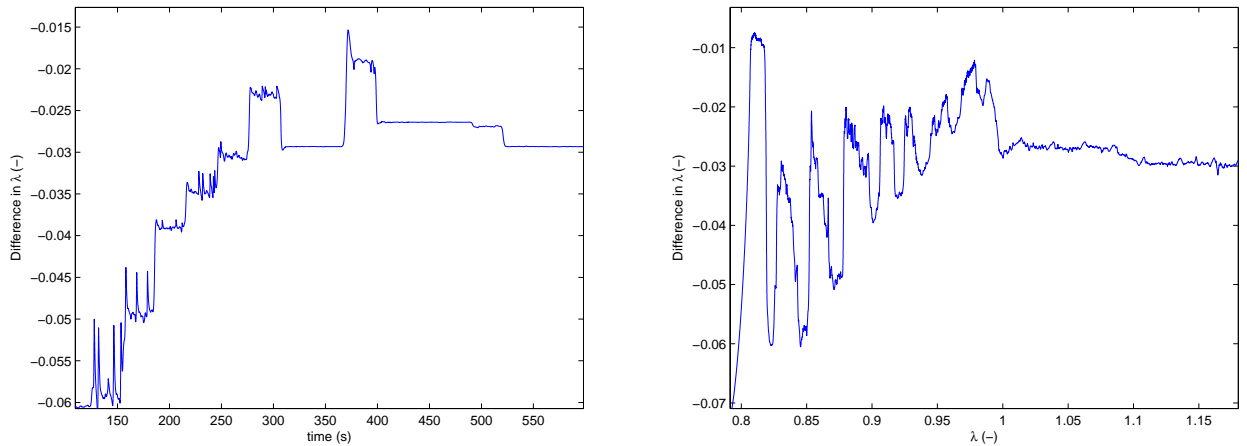


Figure 6.6: The Figure shows the difference between two outputs from the wide band model, which differs in that one has an modeled air leak. The left displays the difference in the time domain and the right the λ -domain

1. When a switch occur save the value from the wide band lambda sensor
2. Assume $\lambda = 1$ when switch occurs and calculate offset
3. Check if offset is sensible
4. Don't use the offset directly but instead let it influence, together with the old offset, the new offset

The switch detection is simple and works like in the observer model. To check if the offset is sensible the least deviant, compared with the running offset, from a number of offsets is used. This offset is then shifted into a shift register. In Figure 6.13 the output can be seen from the Running Average Model during a test. The switch type input is during the entire test fed with a continuously switching signal. This makes the observer's output approaches $\lambda = 1$ irrespective of what the value really is. This model was also tested in the real engine test setup. Parts of the engine was controlled using RTAI and Simulink with this model. The tests were successfully and the ECU model could be implemented ¹.

6.3.3 Results

Both the models seems to give reasonable outputs, the difference is easily spotted with the discrete step of the running average model. The benefit of the this mode is that it uses only operation easily transformed into memory and if-cases when ported to the ECU code.

6.4 Implemented model

The final implementation follows the running average model with the exception of the sensible offset step (see Table 4). In the ECU an additional step was introduced, when detecting a switch the values before and after the switch can not be too far away from each other. This to further avoid erroneous offset values. In addition an algorithm to force the switch sensor to switch was added, this is called *forced switch mode*. It works by, when the switch sensor indicates lean, enrich the mixture until the switch is found. When the switch sensor indicates rich the opposite procedure is taken. This gets the result that the engine is actually run from the switch sensor, creating a oscillating behavior. This speeds up the offset calculation considerable. The practical details is that a new control mode was added in the ECU. The ability to adapt the sensitivity was also added, when starting the offset calculations the algorithm uses more loose restrictions of what offset values to use. This speeds up the calculation in the beginning, when the offset has started to settle more strict rules are then adapted again. The offset is added before the ECU reads the value making it totally transparent for the ECU.

¹these results are not published any further.

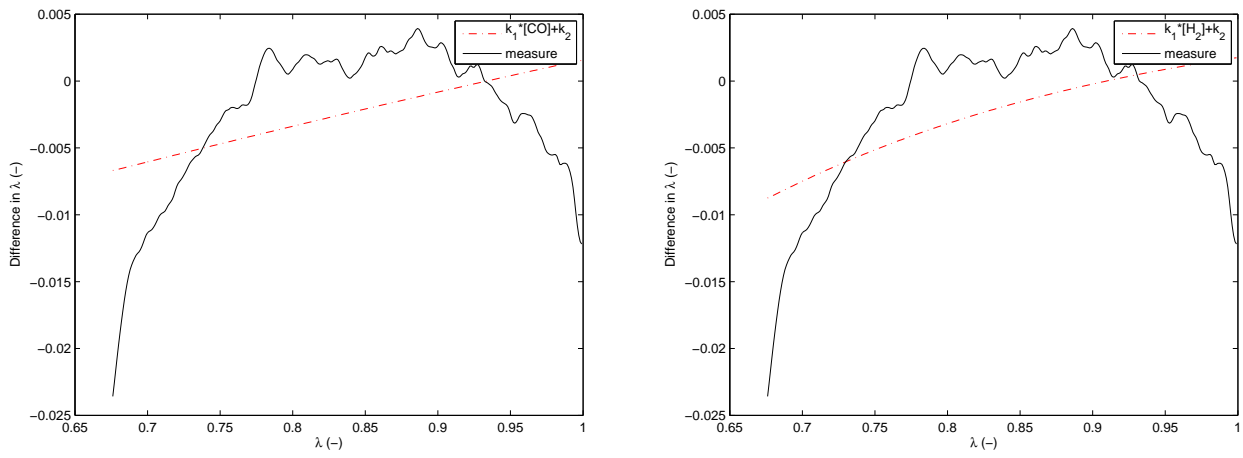


Figure 6.7: The Figures shows the real difference and a fitted curve to the assumption $error = k_1 * [XX] + k_2$. The left Figure is CO and the right is H_2 . Note that the results have been filtered for a better view.

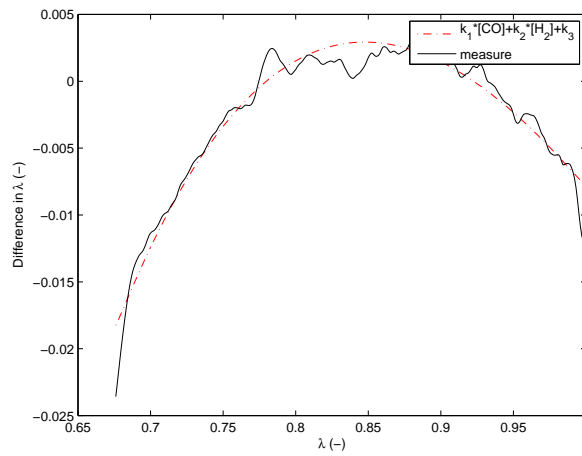


Figure 6.8: The difference error assumed to be on the form $error = k_1 * [CO] + k_2 * [H_2] + k_3$. Note that the results have been filtered for a better view.

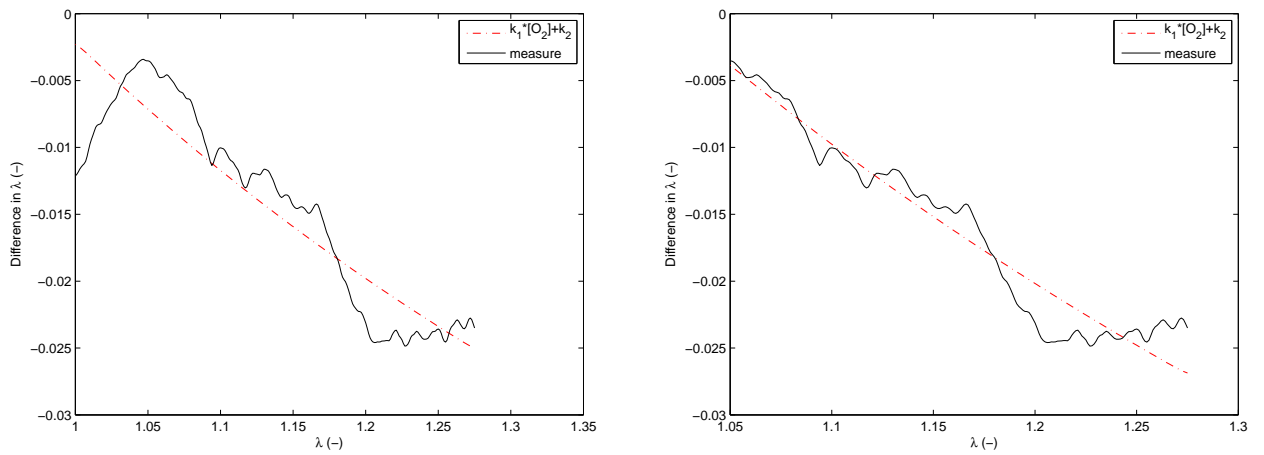


Figure 6.9: The difference error assumed to be on the form $error = k_1 * [O_2] + k_2$. The left Figure is using the entire range $\lambda > 1$ as input to the least square where as the right only uses $\lambda > 1.05$. Note that the results have been filtered for a better view.

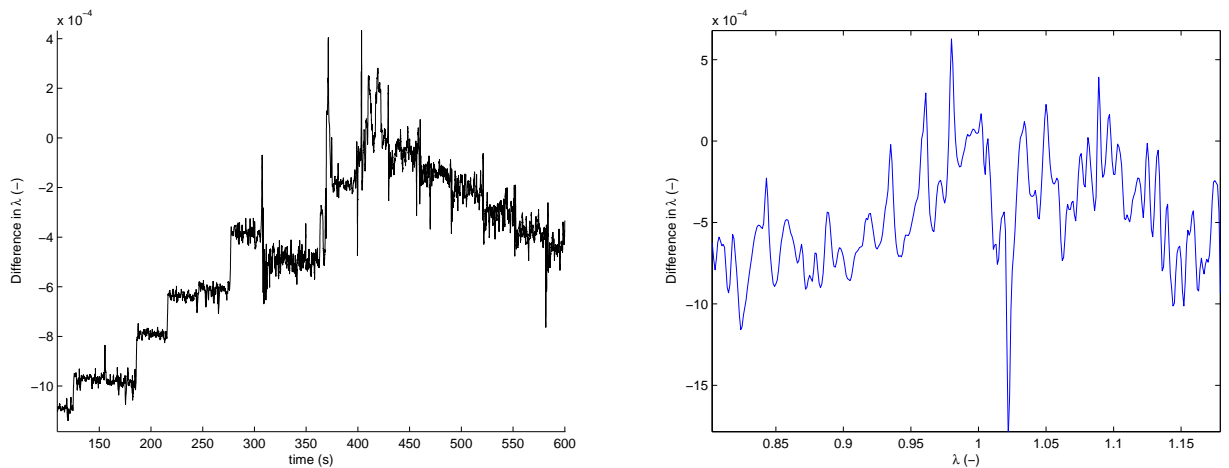


Figure 6.10: The Figure shows the difference between two outputs from the wide band model, which differs on what fuel is injected. One runs on octane and the other runs on octane with 20% ethanol. The left Figure shows the difference in the time domain and the right the difference in the λ -domain

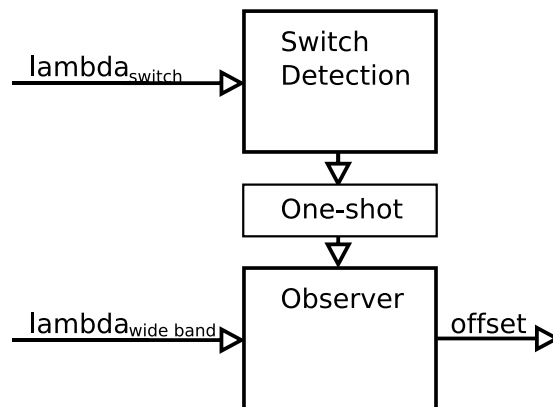


Figure 6.11: The Figure shows an overview of the observer model.

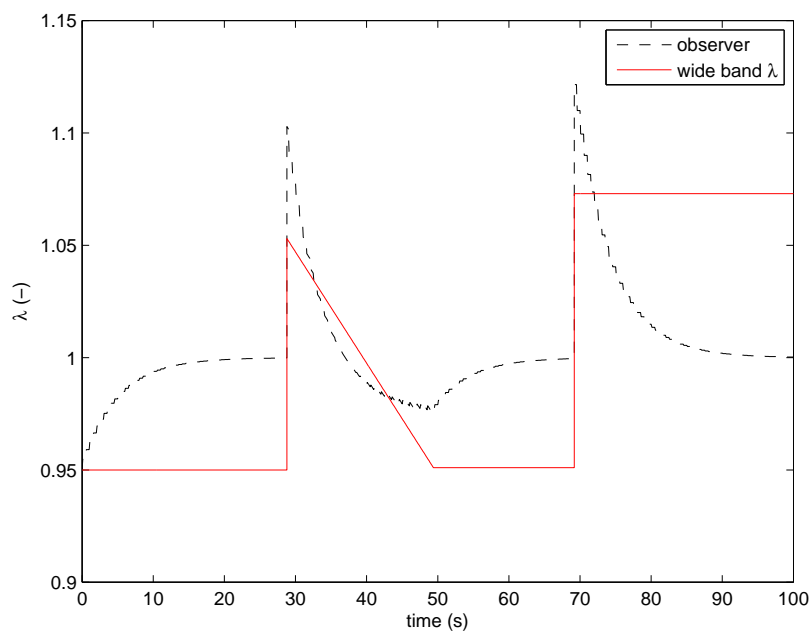


Figure 6.12: Output from the observer together with the wide band input. The switch signal is not seen in the Figure but it is switching constantly, making the observer's output approach $\lambda = 1$.

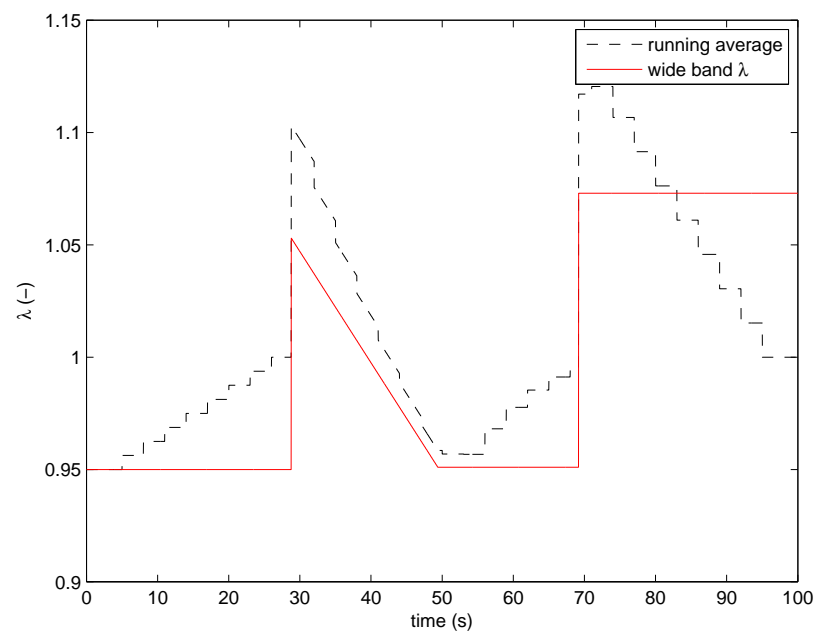


Figure 6.13: Output from the Running Average Model together with the wide band input. The switch signal is not seen in the Figure but it is switching constantly, making the model's output approach $\lambda = 1$.

Chapter 7

Validation of UEGO observer

This chapter describes test results from using the UEGO observer implemented into the ECU. Unfortunately the tests are not performed with the same two lambda sensors as the preceding chapter describes (see Section 6.1). Although the two sensors used in this chapter have a similar difference.

7.1 Adaption

To test the observer the engine is held at an approximately constant RPM and the throttle is adjusted slightly up and down to create variations in lambda. This is demanded to get the switch type sensor to switch. The output from the test can be seen in Figure 7.1. One interesting thing is to see the relation between the two lambda sensors

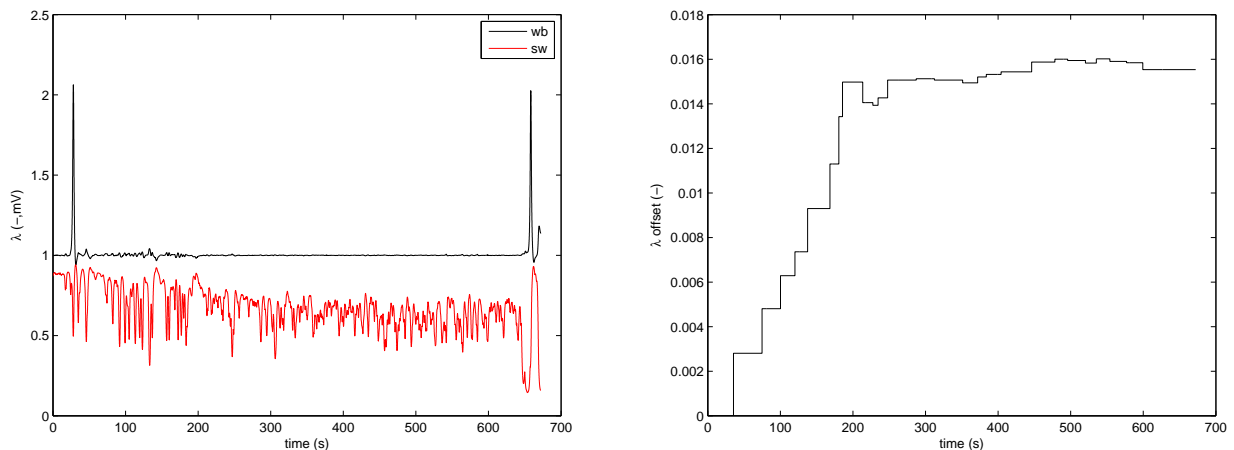


Figure 7.1: A test is performed to validate the adaption, the engine is held at a approximately constant RPM and the throttle is adjusted slightly up and down to create variations in lambda. The right Figure shows the output from the λ -sensors. The left Figure is the resulting offset.

on the engine and the observer's lambda. In Figure 7.2 this can be seen. The one called ETA is an expensive aftermarket sensor and the one called ECU is the engine's original sensor.

7.2 Force lambda swing

To avoid the manual throttle movement, the force lambda swing mode is implemented (see Section 6.4). The result of this mode is that the engine uses the switch type lambda sensor to run the engine, therefore it switches constantly. A simple test, seen in Figure 7.3, is performed letting the RPM be constant and letting the forced lambda swing mode be active in the range 35s – 150s. A complete start of the engine was also tested, see Figure

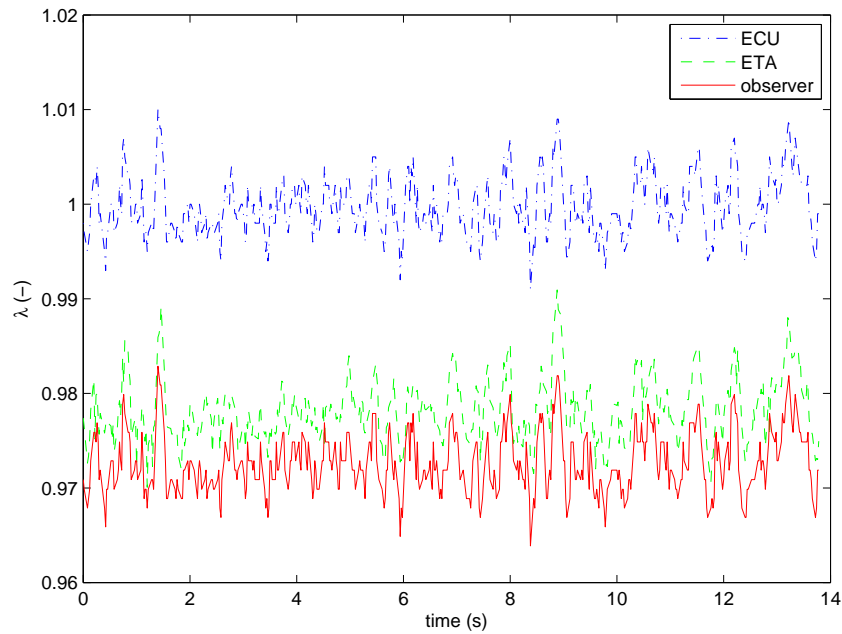


Figure 7.2: The Figure shows the two lambda sensors along with the observer. ETA is an expensive aftermarket sensor and ECU is the original sensor that came with the engine. If the switch type sensor is to be trusted (and thereby the observer) the ETA:s looks most right.

7.4. The forced lambda swing was turned on after approximately 150 seconds.

7.3 Conclusions

All tests showed an calculated offset of around 0.015, which equals the difference between the two sensors. This concludes that one of the wide band sensor must be correct at $\lambda = 1$, presupposed that the switch sensor is right. As the error is much more complicated than an offset a good question is if any improvements were made. A quick test is to take the two lambda sensors from Section 6.1. The mean error before the observer is -0.0121 . If one of the sensors is assumed to be right, the new mean is -0.071 . Although the observer only uses an offset error the result is surprisingly good, almost half the error over the entire spectrum and zero error at $\lambda = 1$.

Another conclusion made is that if the offset is saved when shutting down the engine, the force lambda swing might not be needed. When the engine starts the switch sensor switches a few times, this is enough to get a reasonable value of the offset rather quick.

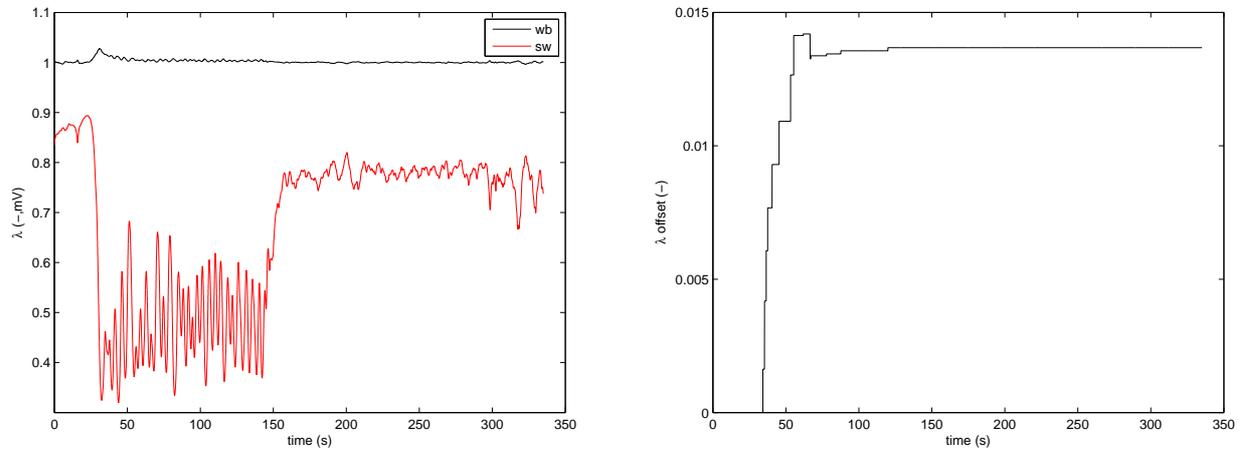


Figure 7.3: A test is performed to validate the forced lambda swing mode, the engine is held at approximately constant RPM and the mode is active during $35s - 150s$.

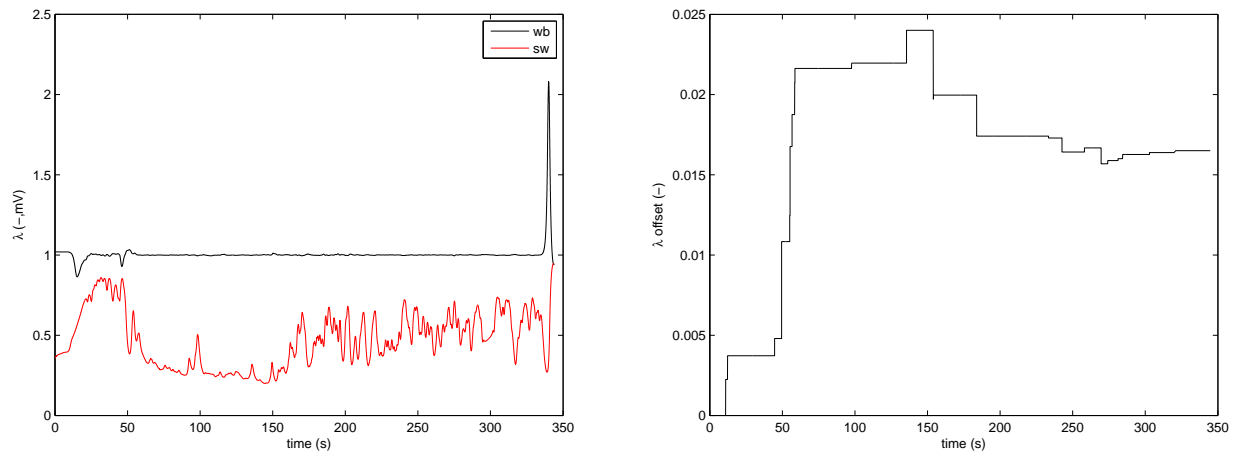


Figure 7.4: This Figure shows the result when adapting from engine start. The forced lambda swing was turned on after approximately 150 seconds.

Chapter 8

Final thoughts and Conclusions

Although the wide band lambda sensor is a very complex sensor it is shown that it can be understood with simple mathematics and basic knowledge in chemistry. One conclusion drawn from the development of the model is that sensor is, on the lean side, mainly Oxygen driven and on the rich side the sensor is mostly sensitive for Carbon Oxide and especially Hydrogen. Furthermore no gas alone can describe the sensor accurately, this retires the term oxygen sensor.

8.1 Correctness of UEGO model

The developed model agrees well with the real sensor for steady state conditions. For transient conditions the model needs to be refined further. A great thing with the model is that it only contains very simple equations, this means that it can be utilized in systems with very low processing power. In addition the test values used are from *after* the catalytic converter, this is harder to model because before the catalytic converter the concentration of *CO* correlates to H_2 for a specific lambda. After the catalytic converter there is no such reliable relation making it harder to get an unified model. The pressure effect on the sensors is indistinct, the model states more pressure more swing but in reality it doesn't seem that simple. The conclusion drawn is that the diffusion into the sensor is mainly not pressure driven.

8.2 Guidelines for a optimal UEGO

When building a lambda sensing device the controller is of equal importance as the sensor element itself. This is due to the sensitivity of surrounding factors that the controller must be able to handle. For coping with temperature sensitivity a good temperature controller should be used, furthermore a temperature compensation should be implemented. This for when the temperature controller cannot guarantee a correct temperature, for example during an overtake. The pressure effect must also be considered, at least if the controller is suppose to be used at $\lambda \neq 1$. Best of all is to have a pressure sensor incorporated into the lambda sensor. If a pressure sensor is used smart calculations can be utilized with the Brettschneider equation to calculate lambda. With this the sensor gets easily portable to other systems/places.

8.3 Guidelines for an optimal use

When using a UEGO, care should be taken not to employ the sensor in an environment which it wasn't designed for, at least not without a re-calibration. Pressure effects and gas sensitivity can destroy the output. To be exact, also the same type of fuel must be used as when the calibration is made. Care should also be taken with the calibration resistor.

8.4 Differing lambda

As for the differing wide band λ -sensors tested, gas sensitivity is the reason that comes closest to explain the difference. A better gas model is needed to investigate further. The explanation for the different sensitivities could

be one or more of the following aspects: The nernst cell could be different, the pump cell could be differently good to pump out different gases between the two sensors or even the diffusion step could be responsible. This cannot be explained without going into details of the different sensors.

8.5 Observer

As the true origin of the differing lambda sensors remains unsolved a simple offset is assumed for the observer. As the error is much more complicated in real life a good question is if any improvements was made. A quick test is to take the two lambda sensors from Section 6.1. The mean error before the observer is -0.0121 . If one of the sensors is assumed to be right and the developed observer is used, the new mean is -0.071 . Although the observer only uses an offset error the result is surprisingly good, almost half the error over the entire spectrum and zero error at $\lambda = 1$.

References

- [1] Bridge analyzers. Lambda calculation - the bretttschneider equation, general principles and methods. Jun 2003.
- [2] Per Andersson. *Air charge estimation in turbocharged spark ignition engines*. PhD thesis, Linköpings Universitet, 2005.
- [3] Theophil Sebastian Auckenthaler. *Modelling and Control of Three-Way Catalytic Converters*. PhD thesis, July 2005.
- [4] Bosch. Oxygen sensors. May 2001.
- [5] Grippo Bowling. Precision wideband controller. October 2005.
- [6] Yunus A Cengel and Robert H. Turner. *Fundamentals of Thermal-fluid sciences*. McGraw Hill, 2005.
- [7] Barbara Freese. *Coal: A human history*. 2004.
- [8] John B. Heywood. *Internal Combustion Engine Fundamentals*. McGraw-Hill series in mechanical engineering. McGraw-Hill, 1992.
- [9] Mikaela Waller Jenny Johansson. Control oriented modeling of the dynamics in a catalytic converter. Master's thesis, Linköpings Universitet, 2005.
- [10] James C. Peyton Jones. Modeling combined catalyst oxygen storage and reversible deactivation dynamics for improved emissions prediction. Jan 2003.
- [11] James C. Peyton Jones and Kenneth R. Muske. A novel approach to catalyst obd. Jan 2005.
- [12] David Long. Turbo upgrade for vg30dett. <http://cherrypicker.tripod.com>, Sep 2006.
- [13] Lars Nielsen and Lars Eriksson. *Vehicular Systems*. Bokakademin, 2005.
- [14] DigiTimes.com Shaun Chen, Taipei; Rodney Chan. Car electronics to account for 50percent of production costs by 2015. July 2006.
- [15] H. Geering T. Auckenthaler, C. Onder. Aspects of dynamic three-way catalyst behaviour including oxygen storage. 2004.
- [16] C.Schnabel V. Hackel and A. Tiefenbach. Wide band oxygen sensor electronic control unit (lambdatronic). Technical report, Jan 2005.
- [17] Wikipedia. Automobile. <http://en.wikipedia.org/wiki/Car>, May 2006.
- [18] Wikipedia. Medical information. <http://www.merck.com/mmhe/>, May 2006.
- [19] Wikipedia. Nikolaus otto. <http://en.wikipedia.org/wiki/NikolausOtto>, May 2006.

List of Figures

1.1	Exhaust gases	3
1.2	CO emissions	4
1.3	HC emissions	4
1.4	NOx emissions	5
1.5	Lambda sensor	6
2.1	Engine overview	8
2.2	Operation of a four-stroke engine	8
2.3	The intake side of an engine	9
3.1	Placing of the lambda sensor	11
3.2	Typical output from a switch type lambda	12
3.3	Typical output when using a switch type lambda	13
3.4	Physical structure of a planar switch type sensor	14
3.5	Output from a switch type sensor with different temperatures	15
3.6	Typical output from a wide band λ -sensor	16
3.7	Physical structure of a wide band sensor	16
3.8	Electrical structure of a wide band sensor	17
4.1	Wide band model	18
4.2	Output from exhaust gas model	20
4.3	Gas concentrations for first set of data	22
4.4	Oxygen based model 1	23
4.5	Oxygen based model 2	24
4.6	Extended gas model	25
4.7	Structure of full Auckenthaler model	25
4.8	Auckenthaler result	26
4.9	Simplified Auckenthaler result	27
4.10	Simplified Auckenthaler with diffusion	28
4.11	Linear regression model with cheating	29
4.12	The diffusion's effect on CO concentration	30
4.13	Concentration difference	31
4.14	The change in partial pressure for a ramp in current	32
4.15	Lookup table	32
4.16	Lookup error table	33
5.1	test 1 of uego model	35
5.2	test 2 of uego model	36
5.3	Pressure comparison	37
5.4	Pressure test	38
6.1	Difference between the two lambda sensors	40
6.2	R_{cal} use	41
6.3	R_{cal} error	41
6.4	Pressure difference for the two lambda sensors	42

6.5	Pressure error	43
6.6	Air leak error	44
6.7	Gas sensitivity error CO H2	45
6.8	Gas sensitivity error CO plus H2	45
6.9	Gas sensitivity error O2	46
6.10	fuel error	46
6.11	Structural view over observer	47
6.12	Output from observer	47
6.13	Output from running average model	48
7.1	Adaption	49
7.2	Different lambda sensors	50
7.3	Adaption with forced lambda swing	51
7.4	Adaption during start	51
A.1	Gas concentrations for first set of data	59
A.2	Gas concentrations for second set of data	60
A.3	Gas concentrations for third set of data	61

List of Tables

1.1	Introduction years of Europeans emission standards	5
1.2	Limits for different emission standards	6
4.1	Resulting concentrations exhaust gas model	20

Appendix A

Data

This appendix describes the test available for the thesis.

A.1 Problems with test data

Unfortunately no data perfectly suited could be founded for this thesis. The data found in [15] is not a perfect match, this is not very surprising as the intention with the data was completely different than what it has been used for in this thesis. Two main problems can be discern:

- The model developed in this thesis was ment to be for a uego in front of the catalytic converter but the data collected is after the converter.
- The second problem is that it seems that the data has quite low resolution, this is a major problem because the models that we are going to develop is quite sensitive for some components. As always interference a problem but as the exact test setup is unknown no compensation can be made. This makes it really hard to filter out *real* data.

A.2 Structure and data

Figure A.1,A.2 and A.3 shows the gas concentrations for their respective test run. Also seen is the output from the λ -sensors.

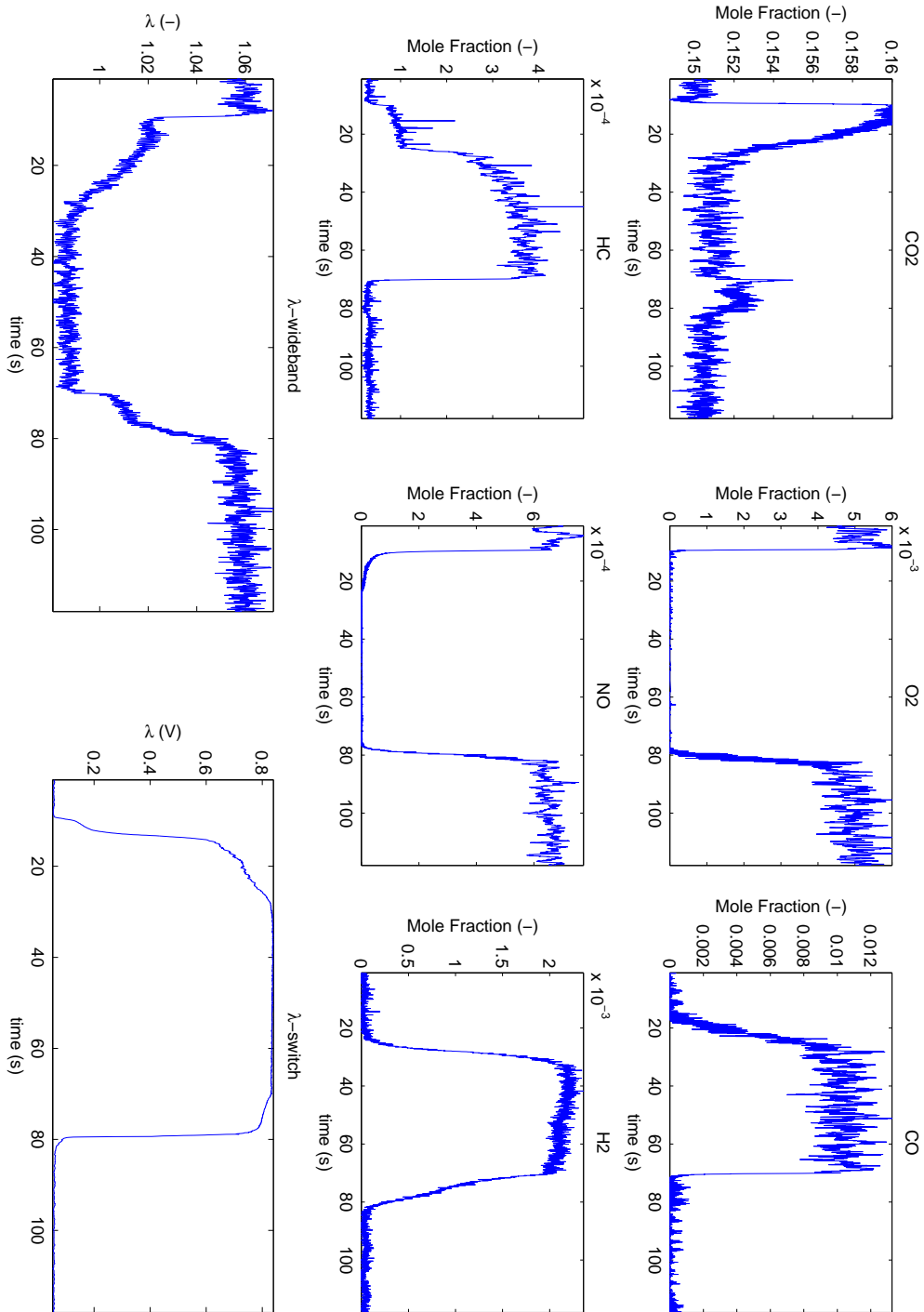


Figure A.1: Gas concentrations for first set of data

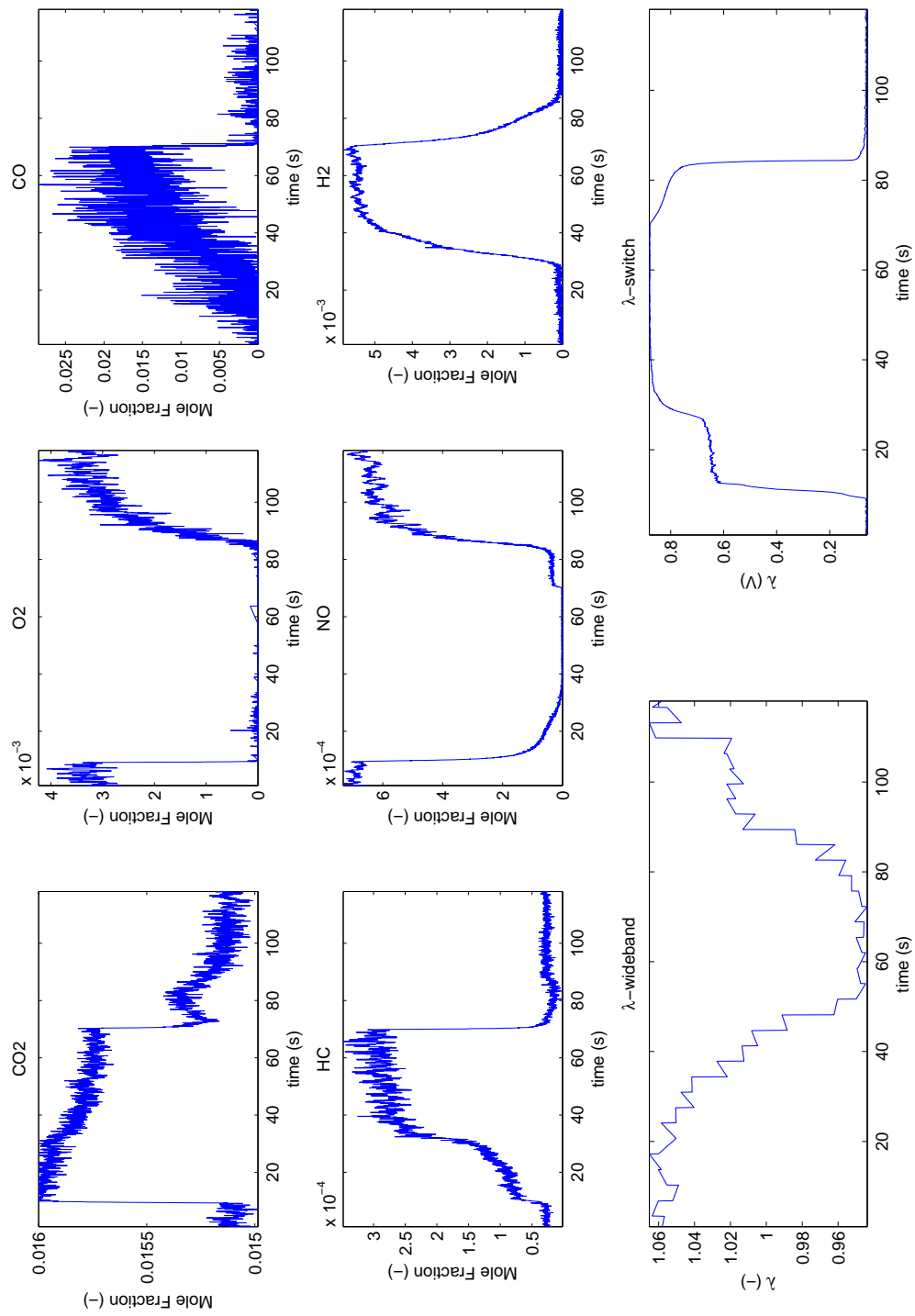


Figure A.2: Gas concentrations for second set of data

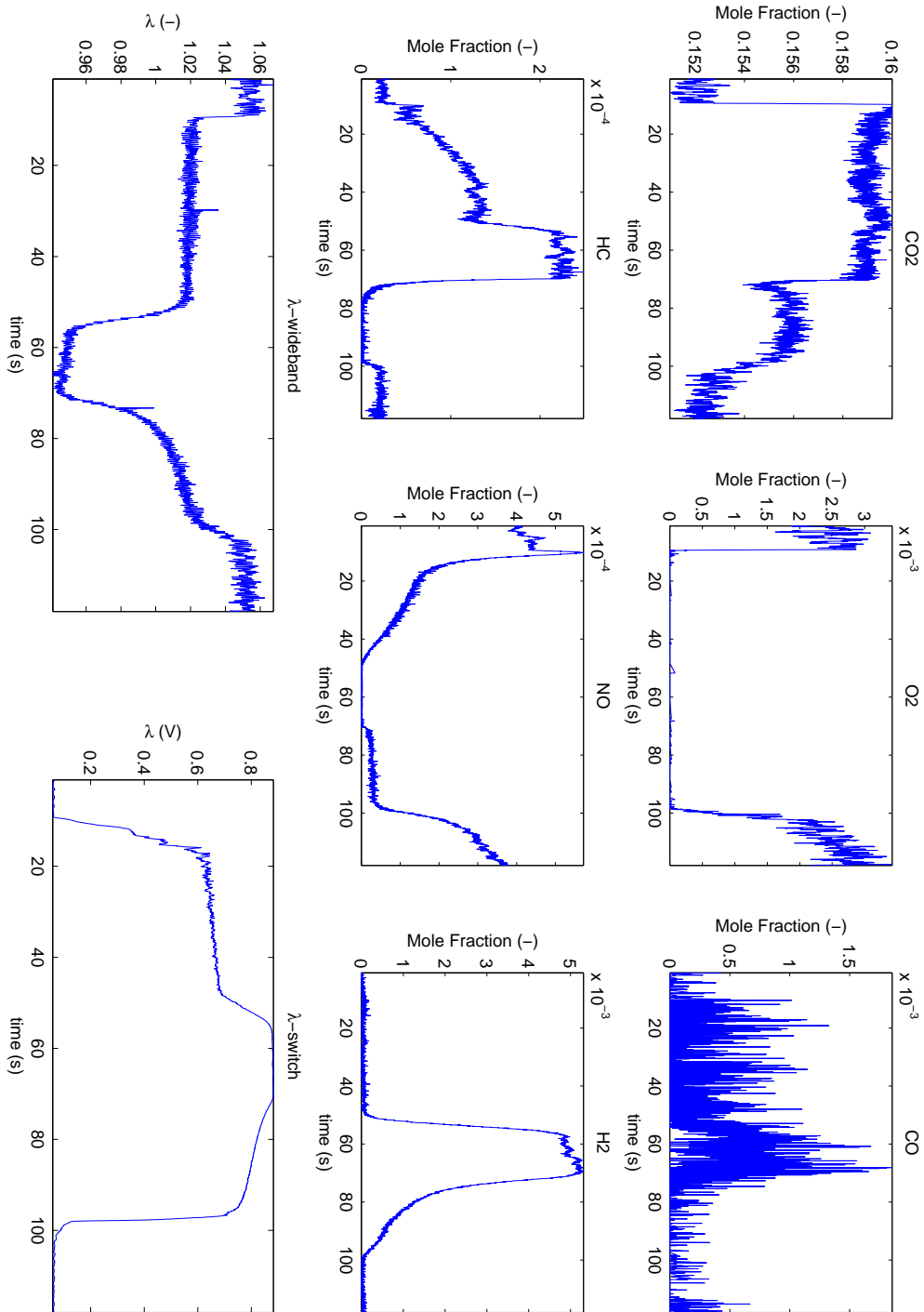


Figure A.3: Gas concentrations for third set of data

Appendix B

Calculated values

Here all calculated values can be found.

Oxygen based model

$$k_2 = 0.23359$$

$$k_3 = 3.54639e + 02$$

$$k_4 = 9.99579e + 03$$

Oxygen based model2

$$k_2 = 0.82641$$

$$k_3 = 5.161471e + 01$$

$$k_4 = -5.60595e + 03$$

Extended gas model

$$k_{0'} = 0.5561$$

$$k_{1'} = 102.1526$$

$$k_{2'} = 78.0325$$

$$k_{3'} = 12.6688$$

Simplified Auckenthaler with diffusion 1

$$diffK = 1.8477$$

Simplified Auckenthaler with diffusion 2

$$diff_{O_2} = 1.1226$$

$$diff_{CO} = 1.2454$$

$$diff_{H_2} = 3.1752$$

Linear model with cheating

$$k_0 = 0.1701$$

$$k_{O_2} = -22.8556$$

$$k_1 = 0.7146$$

$$k_{H_2} = 43.2916$$

$$k_{CO} = 3.2747$$

Oxygen Pump

$$k_{CO} = 2/2$$

$$k_{H_2} = 11/60$$

Regulator

$$k_P = 0.5$$

$$k_I = 1$$

Lambda generation

real test values: $[-0.0900.0180.037] \Rightarrow [0.9861.0221.051.058]$

synthetic gas model: $[-0.8168-0.6059-0.25791.14e-30.13320.2099] \Rightarrow [0.83390.86780.935611.10511.1729]$

Copyright

Svenska

Detta dokument hålls tillgängligt på Internet - eller dess framtida ersättare - under en längre tid från publiceringsdatum under förutsättning att inga extra-ordinära omständigheter uppstår.

Tillgång till dokumentet innebär tillstånd för var och en att läsa, ladda ner, skriva ut enstaka kopior för enskilt bruk och att använda det oförändrat för ickekommersiell forskning och för undervisning. Överföring av upphovsrätten vid en senare tidpunkt kan inte upphäva detta tillstånd. All annan användning av dokumentet kräver upphovsmannens medgivande. För att garantera äktheten, säkerheten och tillgängligheten finns det lösningar av teknisk och administrativ art.

Upphovsmannens ideella rätt innefattar rätt att bli nämnd som upphovsman i den omfattning som god sed kräver vid användning av dokumentet på ovan beskrivna sätt samt skydd mot att dokumentet ändras eller presenteras i sådan form eller i sådant sammanhang som är kränkande för upphovsmannens litterära eller konstnärliga anseende eller egenart.

För ytterligare information om Linköping University Electronic Press se förlagets hemsida: <http://www.ep.liu.se/>

English

The publishers will keep this document online on the Internet - or its possible replacement - for a considerable time from the date of publication barring exceptional circumstances.

The online availability of the document implies a permanent permission for anyone to read, to download, to print out single copies for your own use and to use it unchanged for any non-commercial research and educational purpose. Subsequent transfers of copyright cannot revoke this permission. All other uses of the document are conditional on the consent of the copyright owner. The publisher has taken technical and administrative measures to assure authenticity, security and accessibility.

According to intellectual property law the author has the right to be mentioned when his/her work is accessed as described above and to be protected against infringement.

For additional information about the Linköping University Electronic Press and its procedures for publication and for assurance of document integrity, please refer to its WWW home page: <http://www.ep.liu.se/>

© Thommy Jakobsson
Linköping, January 4, 2007